View metadata, citation and similar papers at core.ac.uk

brought to you by CORE

provided by Open Archive Toulouse Archive Ouverte

Open Archive Toulouse Archive Ouverte (OATAO)

OATAO is an open access repository that collects the work of Toulouse researchers and makes it freely available over the web where possible.

This is an author-deposited version published in: http://oatao.univ-toulouse.fr/
Eprints ID: 10802

To cite this document: Le Bihan, Bastien and Kokou, Pierre and Lizy-Destrez, Stéphanie *Computing an optimized trajectory between Earth and an EML2 halo orbit.* (2014) In: AIAA - Scitech, 13 January 2014 - 17 January 2014 (National Harbor, Maryland, United States).

Any correspondence concerning this service should be sent to the repository administrator: staff-oatao@inp-toulouse.fr

Computing an optimized trajectory between Earth and an EML_2 halo orbit

Bastien Le Bihan, Pierre Kokou, and Stéphanie Lizy-Destrez

ISAE Supaero, Toulouse, 31400, France

According to the Global Exploration Roadmap, which reflects the international effort to define feasible and sustainable exploration pathways to the Moon, near-Earth asteroids and Mars, the next step for manned space exploration is the Moon as second home in the Solar System. In that perspective, the Earth-Moon Libration points (EML points) have been a topic of great interest in recent years since EML_1 and EML_2 were suggested as advantageous locations of space hubs in the Moon neighborhood. To materialize this vision, detailed studies are needed to investigate transfers between Earth and the vicinity of EML_2 and the strategies to reduce associated maneuver costs. This work is framed within the perspective of a future deep space habitat in halo orbit around EML_2, and this paper intends to provide quantitative results so as to select the best deployment scenario of the station. The main purpose is to determine the best transfer trajectory between a low-Earth orbit and a halo orbit around EML_2 in terms of cost and duration. Two different kinds of attractive transfer strategies have been identified. Station deployment and cargo missions would use Weak Stability Boundary (WSB) trajectories whereas manned flights would exploit a fly-by strategy as it shows an advantageous compromise between short trip duration and efficiency.

I. Introduction

Since the Apollo program, mankind has not ventured further into space than the close vicinity of Earth. We tried to increase our mastering of Low-Earth Orbits (LEO) and succeeded thanks to several space stations such as Salyut, Skylab, Mir and the International Space Station (ISS). Today, even private spaceships can access LEO and the ISS.

Space exploration and the presence of humans in space is now at a turning point of its history. Nowadays, space agencies build partnerships and lead common studies, such as the International Space Exploration Coordination Group (ISECG), to determine what the future of space exploration will be. They all agree to say that the main objective of upcoming decades will be to send humans to Mars. But considering the current resources, level of technology and political will, we are not capable of doing it yet. A step-by-step development program of spatial activities is needed.

Several scenarios, such as those reported in the Global Exploration Roadmap of ISECG [1], are proposed. Some suggest to go back to the Moon first, others to visit asteroids. But in either case, the deployment of a deep-space habitat in the vicinity of an Earth-Moon Lagrangian (EML) point, whose nature will be explained hereunder, has been pointed out as a key-point milestone to further development of future space technologies.

A station in halo orbit around EML_2 [2] has many advantages: it can serve as a gateway to other promising destinations (Moon, asteroids, Mars...) in the solar system, being linked to them by low-cost passageways. Set up on an appropriate EML_2 halo orbit, the deep-space habitat can maintain continuous line-of-sight communications between Earth and the far side of the Moon [3, 4]. The far side, which would be easily available for the first time in manned flights history, has been suggested as an advantageous location for a radio observatory, as it would be protected from interference with Earth. The absence of spatial debris and of the terrestrial inhomogeneous gravitational field makes a cheaper station-keeping strategy possible.

Classical approaches to spacecraft trajectory design have been quite successful in the past years with Hohmann transfers for the Apollo program but these missions were very costly in terms of propellant. The fuel requirements of these transfers would make the deployment of a massive space station in deep space

unfeasible. However, a new class of low-energy trajectories have been discovered and extensively investigated in recent years. These trajectories take advantage of the natural complex dynamics arising from the presence of a third body (or more bodies) to reduce transfer costs.

The aim of this paper is to identify, among these methods, optimized transfers for station deployment or cargo missions and manned flights, linking a departure low-Earth orbit to the halo orbit of the station. The selection of strategies will be based on two main criteria: the total fuel consumption required to perform the transfer and the time of flight.

Section II introduces the theoretical bases of the dynamics required to carry out this study. It describes the model commonly used to compute low-energy trajectories. Section III provides an overview of the transfer strategies identified in the literature. Section IV develops the family of trajectories chosen for manned missions whereas Section V analyses station deployment and cargo mission scenarios. Section VI presents the conclusions and prospects that can be drawn from this research work.

II. Mathematical background

This section outlines the dynamic model used to study the motion of a spacecraft under the gravitational effect of two massive bodies, within the framework of an Earth-Moon transfer. The mathematical model used to represent the Earth-Moon or Sun-Earth dynamical environments, that is, the Circular Restricted Three-Body Problem (CR3BP), is developed. This model is used to introduce the notions of libration points, libration orbits and invariant manifolds. The CR3BP is commonly used to produce quick and efficient quantitative results for transfers between Earth and libration orbits [4–6].

II.A. Circular Restricted Three-Body Problem

II.A.1. Model

The CR3BP describes the motion, under the gravitational attraction of two massive bodies m_1 and m_2 in circular coplanar motion around their common center of mass, of a particle of negligible mass m_3 (the third body). The two main bodies are often called the primaries. For the purpose of this study, the CR3BP will be used to describe both the Sun-Earth-Spacecraft and Earth-Moon-Spacecraft systems. The motion of the third body is commonly defined in the rotating reference frame centered at the center of mass of the system (see figure 1a). The units of the systems are normalized in the following way: the distance between the primaries, the modulus of their angular velocity and the total mass are equal to 1. The position and velocity of the third body $\bar{x} = \{x, y, z, \dot{x}, \dot{y}, \dot{z}\}$ are then governed by the system of equations [7]:

$$\begin{cases} \ddot{x} - 2\dot{y} &= -\bar{U}_x \\ \ddot{y} + 2\dot{x} &= -\bar{U}_y \\ \ddot{z} &= -\bar{U}_z \end{cases} \tag{1}$$

Where :

$$\begin{aligned} \bar{U}(r_1, r_2) &= -\frac{1}{2}\left[(1-\mu)r_1^2 + \mu r_2^2\right] - \frac{1-\mu}{r_1} - \frac{\mu}{r_2}, \\ r_1^2 &= (x+\mu)^2 + y^2 + z^2, \\ r_2^2 &= (x-1+\mu)^2 + y^2 + z^2, \\ \mu &= \frac{m_2}{m_1 + m_2}. \end{aligned}$$

Here μ is the mass ratio of the primaries, $\bar{U}$ is the effective potential of the system, and r_1 and r_2 are equal to the distance from the third body to the larger and smaller primaries, respectively (see Figure 1a).

System (1) admits an energy integral of motion [8], commonly used in the form of the Jacobi integral, defined as:

$$C(x, y, z, \dot{x}, \dot{y}, \dot{z}) = -2\bar{U} - \left(\dot{x}^2 + \dot{y}^2 + \dot{z}^2\right) \tag{2}$$

Moreover, system (1) is characterized by five equilibrium points, referred to as libration points and denoted with L_i, $i = 1, \ldots, 5$. As shown in figure 1b, the points L_1, L_2, L_3 lie on the line connecting the two primaries and represent collinear configurations, while L_4 and L_5 correspond to equilateral configurations of the masses.

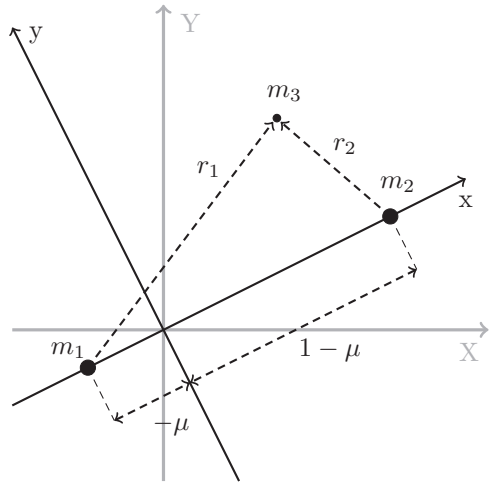

(a) Diagram of the circular restricted three-body problem in normalized units ($\mu = \frac{m_2}{m_1+m_2}$).

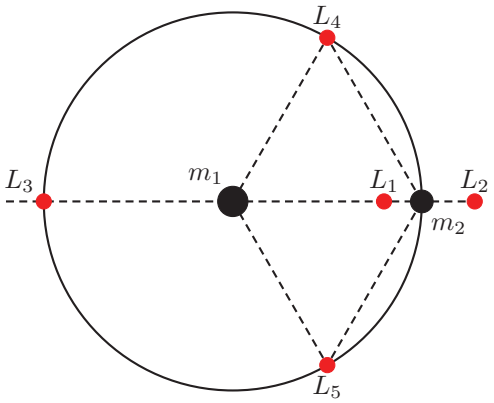

(b) Plot of the equilibrium points of the circular restricted three-body problem in the xy-plane of the rotating reference frame (not to scale).

Figure 1: The Circular Restricted Three-Body Problem

II.A.2. Families of libration orbits

According to literature [7, 9, 10] four different kinds of orbits are known to exist around libration points. They are usually defined as:

- **Lyapunov orbits** are planar periodic orbits in the orbital plane of the primaries (xy-plane). Exact Lyapunov orbits only exist in the CR3BP.
- **Lissajous orbits** are three-dimensional quasi-periodic orbits with an in- and out-of-plane oscillation.
- **Halo orbits** are three-dimensional periodic orbits. Farquhar named them "halo orbits" after the shape they take when seen from Earth [9]. Exact halo orbits can only be computed in the CR3BP.
- **Quasi-halo orbits** are quasi-periodic orbits around a halo orbit. They are intermediate between Lissajous and halo orbits.

For the purpose of this study, focus will be set on halo orbits around EML_2 since it has been previously selected as the most promising location for a possible future deep space habitat [2]. Halo orbits were first computed in the CR3BP and do not exist in a more general model that incorporates additional perturbations. In such a model, differential correction procedures can be used to compute particular Lissajous orbits which are very close to halo orbits for a limited time interval [11].

For a given libration point, halo orbits are divided into two families which are mirror images across the xy-plane. When the maximum out-of-plane amplitude (Az) is in the $+z$ direction, the halo orbit is a member of the northern family (class I) and if the maximum excursion is in the $-z$ direction, the halo orbit is a member of the southern family (class II) [8]. Each member of a family corresponds to a specific Jacobi constant level C. Therefore, halo orbits can be either defined by the couple (class, C) or (class, Az).

To compute a halo orbit, a differential correction scheme with a high order analytical approximation as first guess is commonly deployed [12]. For this study, a third-order approximation developed by Richardson [13] has been used as first guess and a differential correction process has been implemented. Figure 2 shows an example of a southern halo orbit family around EML_2.

II.A.3. Invariant manifold structure associated to libration orbits

For a given northern or southern halo orbit, characterized by its Jacobi constant C_h, one can define the 5-dimensional energy manifold $\mathcal{M}(C_h)$ by:

$$\mathcal{M}(C_h) = \{(x, y, z, \dot{x}, \dot{y}, \dot{z}) : C(x, y, z, \dot{x}, \dot{y}, \dot{z}) = C_h\} \tag{3}$$

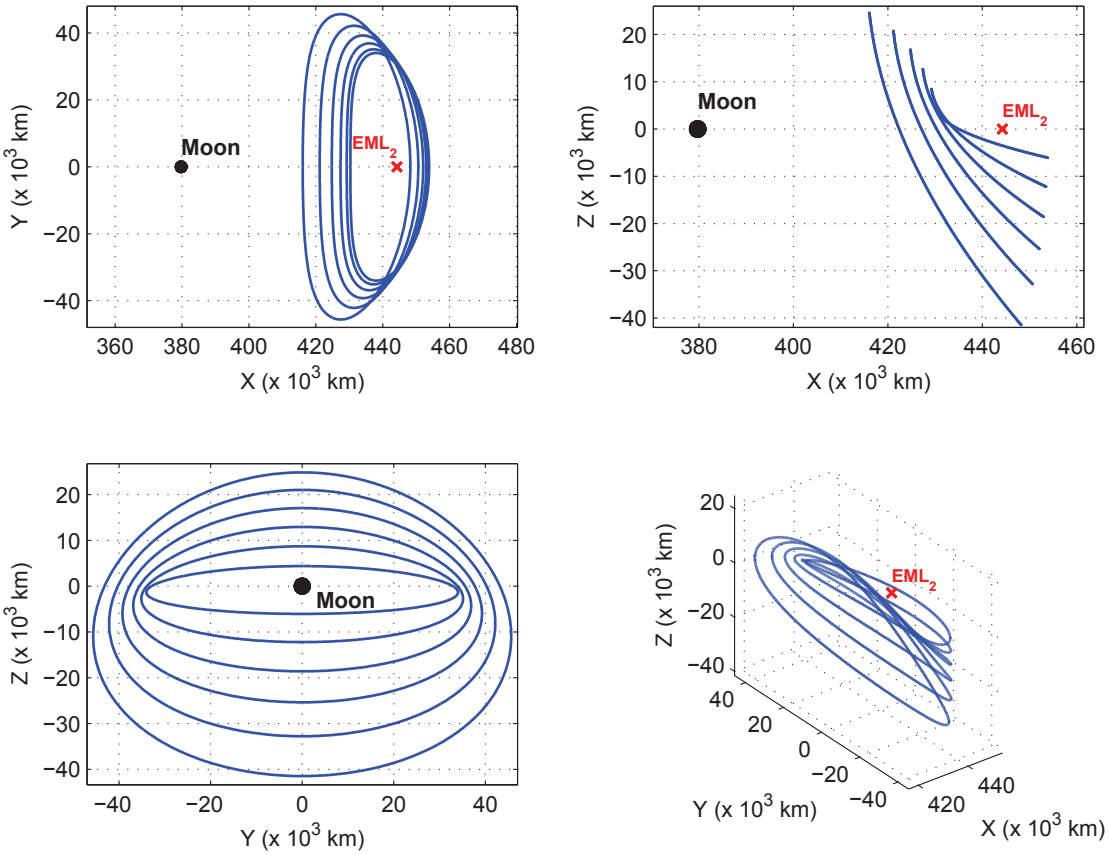

Figure 2: Example of a southern EML_2 halo orbit family, pictured from four perspectives. The Az amplitude ranges from 5000 to 30000 km.

$\mathcal{M}(C_h)$ is embedded in the 6-dimensional phase space $\bar{x} = \{x, y, z, \dot{x}, \dot{y}, \dot{z}\}$.

For a given orbit, the stable (resp. unstable) invariant manifold is defined as the subspace of the 6-dimensional phase space consisting of all vectors whose future (resp. past) positions converge to the periodic orbit. The corresponding trajectories in the vicinity of the halo orbit are often called asymptotic orbits since they slowly converge to or diverge from the halo orbit. Invariant manifolds can be seen as 4-dimensional spaces, topologically equivalent to $S^3 \times \mathbb{R}$ in the 5-dimensional energy manifold $\mathcal{M}(C_h)$. These structures provide dynamical channels beneficial to the design of energy efficient spacecraft trajectories [8]. They are often referred to as "tubes" since they exhibit tube-like shapes when projected onto the 3-dimensional position space.

To compute the invariant manifolds, one can propagate the equations of motion (1). However, given the asymptotic behavior of the motion at arrival or departure, manifolds are not generated directly from a position on the orbit. Usually, a linear approximation of the manifold is calculated for any given point on the orbit using tools from the theory of the dynamical stability of systems. Then, the starting point of the trajectory is taken at a distance d_M in the initial stable or unstable direction given by the linear approximation (see Figure 3a for a visualization of d_M). For further details on the subject, see e.g. [8, 14]. Figure 3b shows an example of the projection onto the position space of the stable and unstable manifolds of an EML_2 southern halo orbit with an amplitude $Az = 5000$ km.

III. Transfer strategies

An extensive bibliographic research has been conducted in order to identify the possible transfer strategies to link a Low-Earth Orbit (LEO) with a halo orbit around EML_2. The framework of this study fits into the context of manned spaceflights. The purpose of this paper is then to find the best trajectories according to two main criteria, the total ΔV required to perform the maneuvers and the time of flight. Using the

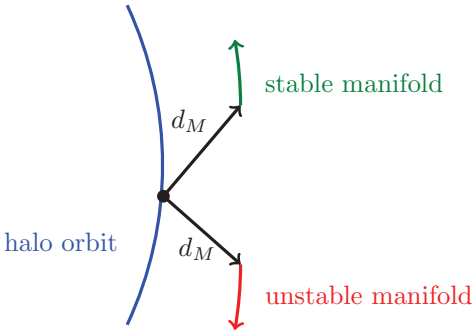

(a) Definition of d_M.

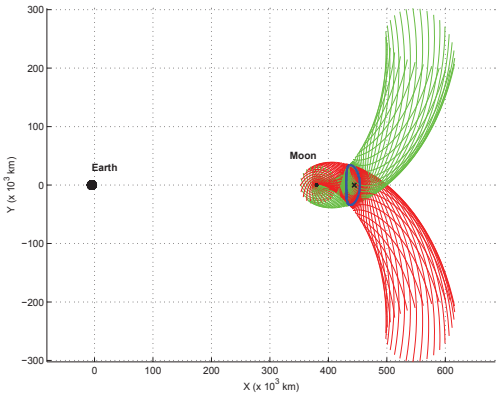

(b) Stable (green) and unstable (red) manifolds of an EML_2 southern halo orbit (blue) with an amplitude $Az = 5000\ km$.

Figure 3: The generation of the stable and unstable manifolds. Their starting point is taken at a distance d_M in the initial stable or unstable direction given by a linear approximation calculated with tools from the theory of the dynamical stability of systems [8].

elements from the previous section, several strategies can be developed so as to minimize the time of flight or the ΔV, or to find an acceptable compromise between these two objectives.

In this section, we will first describe four different strategies and then address the question of return trajectories. Consequently, a comparison between these methods will be made, to finally find the most suitable strategy for the whole life of the station.

For all the methods presented hereunder, costs depend on the strategy itself but also on several other parameters, including:

- A_z, the maximum out-of-plane amplitude in the +z direction of the considered halo orbit, in kilometers. In order to maintain a permanent line of sight with the Earth, this magnitude should be over 3100 km [3].
- h_{LEO} , the altitude of the initial parking low-Earth orbit, in kilometers.
- d_M, the distance between the point on the halo orbit and the actual starting point of the trajectory on the linear approximation of the stable manifold, in kilometers (see Section II.A.3). Its value is usually taken between 50 and 100 km to ensure that the linear approximation remains within the range of validity [8].

III.A. Transfer strategies overview

The principles of the four strategies identified in the literature will now be presented, along with their average time of flight and total required ΔV. The first three strategies fit into the Earth-Moon Three-Body Problem, whereas the last one uses two patched Three-Body problems.

III.A.1. Direct transfer (DT)

The classical method to operate a transfer between two space bodies is a two-maneuver direct ballistic transfer.

This type of transfer does not use at all the manifolds and their insertion properties, which makes it the most fuel-consuming strategy. The ΔV of such a transfer is around **4000 m/s** and requires two maneuvers, one to leave the LEO and the other to slow down when reaching the halo orbit. This is, however, the shortest transfer possible with a time of flight between **3 and 15 days**.

III.A.2. Indirect transfer (IT)

When it comes to reducing the ΔV, other strategies should be developed, such as indirect transfers using the EML_2 stable manifold. With these methods, the objective is to enter the manifold at an optimized point and then follow it toward the halo orbit. The first of these methods consists in generating many entrance points along the manifold in order to select the one which will lead to a minimum ΔV, without any assumption on the position of these entrance points. In other words, the time of flight on the manifold is initially let free to vary.

For each manifold entrance point, the boosts to leave the LEO and to enter the manifold will be different, the main objective being to minimize their sum. Some authors have used this method, generating many entrance points and choosing the best trajectories among their results [5]. With this strategy the total needed ΔV from the LEO orbit to the halo orbit is around **3200-3300 m/s**, but the time of flight increases, between **50 and 150 days** approximately.

Bernelli-Zazzera [15] developed an optimization process for this method with the time of flight on the manifold as a decision variable, using genetic algorithm and sequential programming. Without any additional gravitational assist from the Moon or the Sun, they computed several low-cost trajectories with a ΔV close to 3200 m/s.

III.A.3. Lunar Fly-By transfer (LFB)

In this strategy, the entrance point in the manifold is chosen close to the Moon and is not a free parameter anymore. In this type of transfer, the slingshot effect of the moon is used when the spacecraft enters the manifold. Thus, the key parameters are the altitude of the Lunar fly-by and the angle relative to the Moon with which the spacecraft reaches the manifold.

This strategy leads to a good compromise between the ΔV and the time of flight. Recent publications give ΔV of **3300-3400 m/s** approximately for a time of flight between **10 and 25 days** [4, 6, 16].

III.A.4. Weak Stability Boundary transfer (WSB)

In Weak Stability Boundary strategies, the CR3BP is not enough anymore, and the model should be extended to two patched Three-Body problems to account for the influence of the Sun. The Weak Stability Boundary transfer uses a property of another manifold, the stable one from the Sun-Earth system. In this Sun-Earth 3-body problem, Earth is the smallest primary which makes this manifold come much closer to Earth than the Earth-Moon manifolds. It is then much easier in terms of ΔV to reach this particular manifold and to make use of its rich dynamics in order to reduce the cost. The principle of this strategy is to take profit of the "twisting" properties of trajectories near the Sun-Earth manifold [8] to leave LEO with a first maneuver and then enter the Earth-Moon stable manifold with or without a new maneuver.

This fourth strategy is definitely the cheapest, with values of ΔV around **3100-3200 m/s**. Lasting between **80 and 120 days**, it is also one of the slowest possible transfers.

III.B. Return trajectories

To this point, only Earth-to-Moon trajectories have been discussed, and not the way back. The return trajectories from the halo orbit to LEO can use exactly the same trajectories as described above, provided the roles of unstable and stable manifolds are reversed. Instead of using the stable manifold to asymptotically get to the halo orbit, the unstable manifold will be used.

Moreover, if only the Earth-Moon-spacecraft 3-body problem is considered, the *theorem of image trajectories* [17] can be used. This theorem states that if a trajectory is feasible in the Earth-Moon system, its image relatively to the plane containing the Earth-Moon axis and orthogonal to the plane of rotation of the Moon around Earth is also feasible if flown in the opposite direction. More recent results [18] point out that optimal Earth-Moon and Moon-Earth trajectories are mirror images of one another.

III.C. Strategies comparison

This study aims to identify and describes the best strategies for cargo and manned flights to halo orbit. In this framework, some of the best results in term of fuel consumption and time of flight have been selected in the literature for each method identified in the previous section. We now want to confront and rank them

both for cargo and manned missions. First, the parameters used to identify and compare the trajectories are presented and discussed along with a global comparison table. The maneuver cost of each quantitative result is put into perspective with a theoretical minimum ΔV_{min} based on energy considerations. Finally, the most suitable strategy is selected both for cargo missions and manned spaceflights.

III.C.1. Comparison parameters and results

Table 1 summarizes the comparison of IT, LFB and WSB transfers to the EML_2 halo orbits from several references. The direct transfers (DT) are not discussed here, given their high maneuver cost. The parameters presented in this table are:

- Az, the maximum out-of-plane amplitude in the $+z$ direction of the considered orbit, in kilometers.
- h_{LEO}, the altitude of the initial low-Earth orbit, in kilometers.
- TOF which stands for the Time Of Flight, in days.
- ΔV_{tot}, the total cost of the transfer, in meters per second.
- ΔV_{LEO}, the cost of the Earth escape maneuver, in meters per second.
- ΔV_{Mani}, the cost of the insertion into the stable manifold of the halo orbit, in meters per second.
- The method used: Weak Stability Boundary transfers (WSB), Lunar Fly-By transfers (LFB) and Indirect Transfer (IT).
- The model in which the calculations are led. Four main types of model are used: the Circular Restricted Three-Body Problem (CR3BP), the patched CR3BP, the Bi-Circular Four-Body Problem (BCFBP), and the JPL ephemeris model.

The comparative analysis of Table 1 is made difficult by the differences in terms of dynamical model, low-Earth orbit altitude and halo orbit size. In particular, there is no overall agreement on a reference value for low-Earth orbit altitude even though it has a paramount influence on the resulting ΔV_{LEO}. Despite these limitations, it is still possible to compare results which share the same order of magnitude for every design parameter. Among the results, three comparable ones (in bold) were selected and considered the best results for each strategy. For an indirect transfer and a WSB transfer the time of flight is quite long, and the ΔV around 3150 m/s. On the contrary, the Lunar Fly-By transfer enables the spacecraft to be around EML_2 in 16 days, but costs about 150 m/s more.

III.C.2. Comparison parameters and results

The difficulty of the comparative analysis of Table 1 calls for a shared reference, such as a common lower limit to the ΔV for a transfer from the Earth to EML_2 halo orbits. We can try to estimate the minimum ΔV necessary to carry out such a transfer with a single LEO maneuver in the CR3BP. The calculations of this section are based on the work of [8, 21]. The initial velocity on the Earth orbit is denoted V_{LEO}.

The general idea is to apply a boost ΔV parallel to the LEO velocity in order to maximize the variation of the Jacobi constant in LEO named C_{LEO}. This variation must be such that the new velocity $V_{new} = V_{LEO} + \Delta V$ defines a new Jacobi constant C_{new} which is less or equal to the Jacobi constant C_h on the desired orbit. Hence, setting $C_{new} = C_h$, the minimum theoretical cost is given by:

$$\Delta V^{min} = \left(V_{LEO}^2 - C_h + C_{LEO}\right)^{\frac{1}{2}} - V_{LEO} \tag{4}$$

For a given halo orbit altitude, C_{LEO} and V_{LEO} can be easily derived, e.g. with a Two-Body Problem (2BP) approximation. Then, for a given halo orbit defined by its Jacobi constant C_h, the minimum LEO maneuver required to reach the halo orbit can be calculated. Obviously, some restrictions have to be made about the validity of this study:

- Only one maneuver has been considered, which shades the comparison with multi-maneuver technique such as Lunar Fly-By transfers.

Table 1: Comparison of several types of transfers to the EML_2 halo orbits.

Ref	Az (km)	h_{LEO} (km)	TOF (days)	ΔV_{tot} $(m.s^{-1})$	ΔV_{LEO} $(m.s^{-1})$	ΔV_{Mani} $(m.s^{-1})$	ΔV_{supp} $(m.s^{-1})$	Method	Model
[19]	**8000**	**167**	**98**	**3161**	**3161**	**0**	**0**	**WSB**[b]	**BCRFBP**
[20]	53000	185	110	3196	3196	0	0	WSB	JPL
[20]	53000	185	190	3200	3200	0	0	WSB	CR3BP[e]
[20]	53000	185	110	3264	3264	0	0	WSB	CR3BP[e]
[15]	1000	200	77	3119	–	–	0	IT[c]	CR3BP
[15]	**8000**	**200**	**123**	**3156**	–	–	**0**	**IT**	**CR3BP**
[15]	8000	200	43	3203	–	–	0	IT	CR3BP
[4]	6000	200	20[a]	3440	3060	380	0	LFB[d]	CR3BP
[16]	2000	200	16	3311	3116	193.3	1.9	LFB[f]	JPL
[16]	**5000**	**200**	**16**	**3336**	**3118**	**197.8**	**20.6**	**LFB**	**JPL**
[16]	10000	200	16	3346	3115	189.7	40.8	LFB	JPL
[16]	20000	200	12	3399	3113	179.6	105.7	LFB	JPL
[16]	30000	200	14	3460	3116	186.2	157.6	LFB	JPL
[5]	8000	360	120	3350	3150	200	0	IT	CR3BP
[6]	5000	400	30	3298	3077	216	4	LFB	CR3BP
[4]	6000	500	20[a]	3350	2980	370	0	LFB	CR3BP
[4]	6000	2000	20[a]	3020	2670	350	0	LFB	CR3BP

[a] Average time of flight. The real values lie between 18 and 23 days.

[b] WSB stands for Weak Stability Boundary.

[c] IT stands for Indirect Transfer.

[d] LFB stands for Lunar flyby

[e] The *patched* CR3BP is used: the behaviour of the spacecraft is either evaluated in the Sun-Earth system or the Earth-Moon system.

[f] In this paper, the LFB transfers includes a preliminary boost ΔV_{supp} on the halo orbit to bend the trajectory in the manifold. See the corresponding article for more explanations.

- The relation between the LEO altitude and ΔV^{min} has been implemented in the Earth-Moon CR3BP. In strategies such as WSB transfers, the influence of the Sun naturally lowers the Jacobi constant.
- The initial velocity on the Earth orbit is evaluated in the 2BP approximation, therefore decreasing the pertinence of the derived relation at high altitudes.

Despite these limitations, ΔV^{min} as a function of the LEO altitude may be used as a first approximation of a common lower limit for all the different approaches of Earth-EML_2 transfers. Figure 4 gives an example of the influence of the LEO altitude on ΔV^{min} for two sizes of halo orbits: $Az = 8000\ km$ and $53\ 000\ km$. One can see that the size of the halo orbit has little influence on ΔV^{min} since the maximum variation between the two curves plotted is about 0.3% for the range of altitudes considered, which means between 50 and 550 km. Thus, it is possible to plot several values of Table 1 for comparison, despite their diversity of Az amplitude.

One can see that the lower limit shown on figure 4 is consistent with the literature. One should not expect to find ΔV much lower than the aforementioned theoretical lower limit. Moreoever, the optimization algorithm developed by Bernelli-Zazzera et al. [15] enable them to get very close to the ΔV^{min} for the considered altitude.

III.C.3. Optimized strategy for manned and cargo missions

We aim to select the most suitable strategy for cargo and manned missions to and from halo orbit. Manned spaceflights between Earth and the station requirements are a short time of flight to rapidly access the station and reduce the exposition to radiations in deep space. Figure 5 presents the overall fuel cost ΔV_{tot}

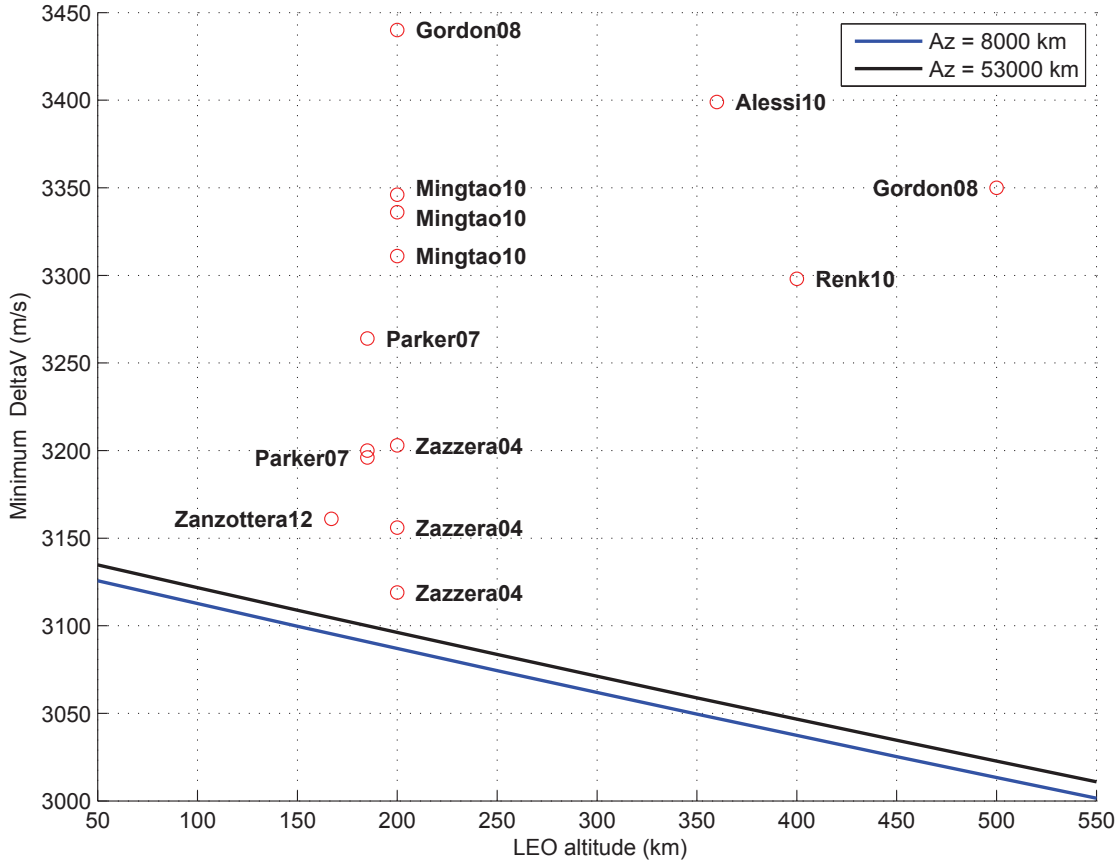

Figure 4: ΔV^{min} as a function of the LEO altitude. Several values from Table 1 (red circles) are plotted for comparison. They are labelled with the convention <Name of the main author, year of publication>.

as a function of the time of flight for the different methods of Earth-EML_2 transfers. One can see that the flyby strategy allows 20-days transfers to EML_2 with a reasonnable cost of 3300-3400 km/s. It has thus been selected as the best compromise for this type of mission.

On the contrary, the main criterion of selection for unmanned flights is the cost reduction in terms of propellant whereas longer trip durations can be accepted. Thus, the Weak Stability Boundary transfers are used as a framework for cargo. Although the approach of Bernelli-Zazzera discussed in III.A.2 deserves to be furtherly developed, it is no longer taken into account, given its uniqueness in the literature [15].

Section IV and V focus on these two choices, in the perspective of their respective type of mission.

IV. Manned transfers trajectories

As stated in the previous section, manned spaceflights between Earth and the station require both a short time of flight and low propellant consumption. Fly-by strategy has been selected as the best compromise for this type of mission. Following the work of [4, 6, 16] and [3], we investigate the influence of the parameters Az, d_M, ϕ on the cost of flyby transfers in terms of time of flight TOF and maneuvers ΔV_{Mani} and ΔV_{LEO}, all variables being defined in Subsection III.C. The goal is to find good trade-offs between the time of flight and the overall fuel cost. Firstly, the strategy, the design parameters and the assumptions used to compute the flyby trajectories are presented. In particular, in the framework of rendezvous with the station, a continuous parametrization of its position is needed. The angular position θ is introduced for this purpose. Then, the variation of the time of flight and amplitude of the maneuvers in relation to the design parameters are studied, and some recommendations for manned spaceflight are presented. Finally, some constraints specific to flyby trajectories are presented in the context of the design of spaceflights from the halo orbit to Earth.

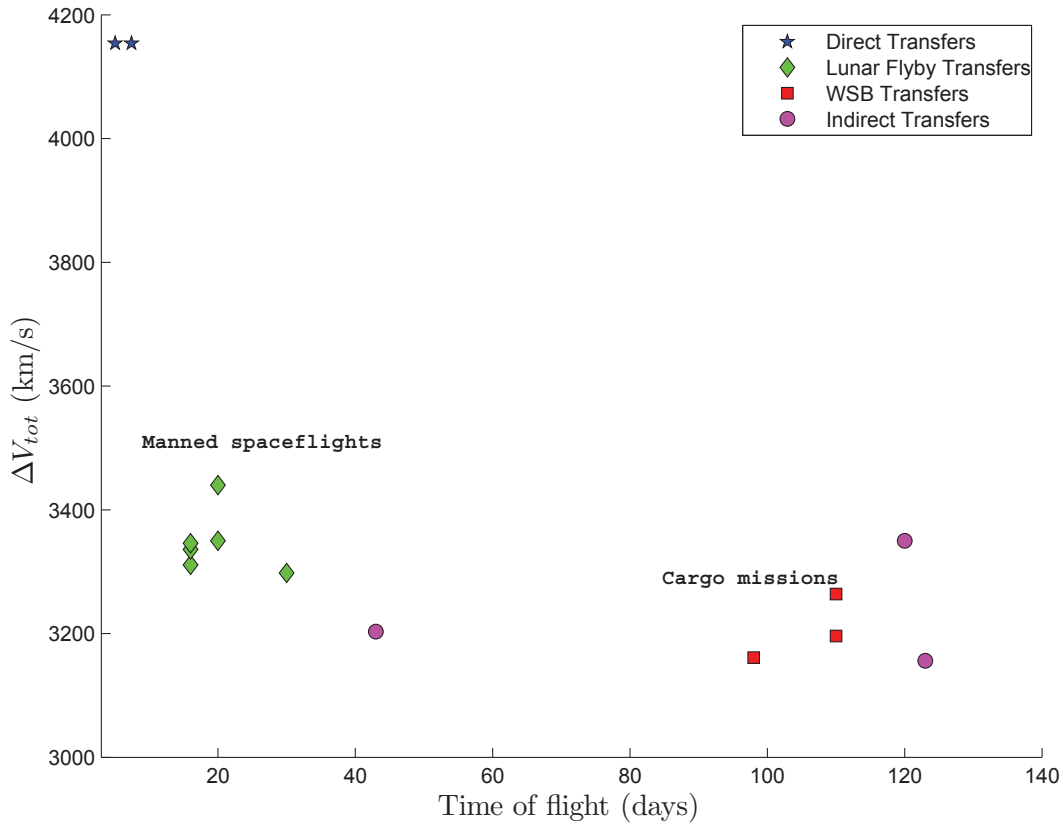

Figure 5: The overall fuel cost ΔV_{tot} as a function of the time of flight for several results in the literature. Several values from Table 1 are plotted, along with examples of direct transfers taken from [6].

IV.A. Strategy and assumptions for the flyby transfers.

The strategy adopted in the present study is a two impulsive LEO-to-halo transfer with a first maneuver ΔV_{LEO} to escape Earth and a second maneuver ΔV_{Mani} in the vicinity of the Moon to inject the spacecraft in the stable manifold of the halo orbit. The arc connecting the low-Earth orbit and the manifold entrance point is noted A_{EM}, the trajectory arc between this point and the halo orbit entrance point is noted A_{MH}. The maneuvers and trajectory branches are schematized in Figure 6. Return trajectories are also considered, with identical notations. In the following subsections, the design parameters of the two types of Earth-to-halo transfers are listed and the numerical differential corrections process used to compute the desired transfers is discussed.

IV.A.1. Parametrization of the position on the halo orbit

Most of the previous efforts on halo orbit transfers chose point numbering to specify the position of departure and arrival on the orbit. However, a continuous parametrization of the position is a necessary step in the broader context of rendezvous with the station. In order to build such a parametrization, the notion of pseudo-center $\bar{X}_{pc}$ of the orbit is here introduced and calculated as follows:

$$\bar{X}_{pc} = \frac{1}{2}\left(\bar{X}_0 - \bar{X}_1\right) \tag{5}$$

where $\bar{X}_0$ and $\bar{X}_1$ are the points of the halo orbit that satisfy $y = 0$ in the Earth-Moon reference frame. These points are plotted in Figure 7, along with the position of the pseudo-center for a given nothern halo orbit with $Az = 5000\ km$.

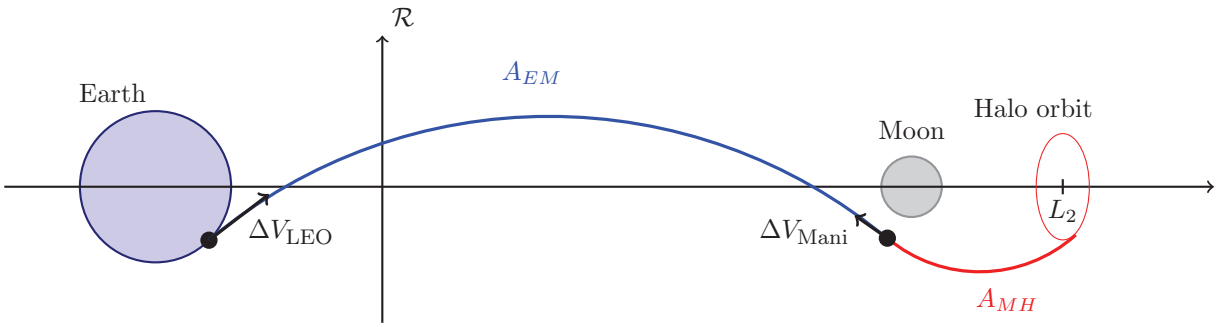

Figure 6: Definition of the maneuvers and arc trajectories in the case of an Earth-to-halo flyby transfer. The trajectory is schematized in the xy-plane of the Earth-Moon reference frame $\mathcal{R}$. A first maneuver ΔV_{LEO} is needed to escape Earth and a second maneuver ΔV_{Mani} in the vicinity of the Moon is required to inject the spacecraft in the stable manifold of the halo orbit. The arc connecting the low-Earth orbit and the Manifold entrance point is noted A_{EM}, the trajectory arc between this point and the halo orbit entrance point is noted A_{MH}.

From the pseudo-center, the angle θ between the ($\bar{X}_{pc}$, $\bar{X}_0$) and ($\bar{X}_{pc}$, spacecraft) directions in the xy-plane is used to parametrize the position of the spacecraft on the orbit. One has to notice that although θ is defined in the xy-plane and not in the three dimensional problem, it uniquely defines the position of the spacecraft. As shown in Figure 7, the angle θ is counted clockwise to follow the natural course of the spacecraft on the orbit.

IV.A.2. Parametrization of the transfers

First of all, as stated in Section II, an EML_2 halo orbit can be defined by its maximum out-of-plane amplitude (Az), and its class (northern or southern orbit). Given the symmetry of the problem with respect to the class, the entire study is led with the northern family, leaving the amplitude **Az** as the only defining parameter of the halo orbit. In this study, values of Az between 4000 km and 30000 km are studied, although special attention is given to low-Az halo orbits since they may yield more cost-efficient transfers [22].

Then, the transfers are separated in two branches A_{EM} and A_{MH}, connected at a specific point in the vicinity of the Moon. The following parameters are used to identify the A_{MH} arc:

- The angle $\boldsymbol{\theta}$ which gives the position of the departure point on the halo orbit. It is taken in the range $[0°, 360°]$. The set (Az, θ) gives a specific position on a given orbit.
- The distance $\mathbf{d_M}$ between the point on the halo orbit and the actual starting point of the trajectory on the linear approximation of the stable manifold. See Subsection II.A.3 and Figure 3a for more details. In the context of numerical simulation, d_M can be considered as a design parameter, despite its non-physical nature [11]. It is taken in the range $[1km, 100km]$ for which the linear approximation is valid. The set (Az, θ, d_M) gives a specific trajectory to/from the halo orbit.
- The angle $\boldsymbol{\phi}$ defined in Figure 8 which defines the connection point between A_{MH} and A_{EM} with respect to the Moon. It is taken in the range $[0°, 90°]$ for Earth-to-halo transfers, and in $[-90°, 0°]$ for halo-to-Earth trajectories. The set (Az, θ, d_M, ϕ) entirely defines the A_{MH} arc and the connection point.

For the A_{EM} arc, the major design parameter is the **altitude** h_{LEO} of the initial low-Earth parking orbit of the spacecraft. The great influence of the LEO altitude on the overall cost is well-known and expected [4, 8, 20], therefore it is fixed to the common value of 200 km to cancel its influence on the results and on the following discussion. The latitude of the parking orbit is let free to vary. Given these assumptions, the A_{EM} arc and the two maneuvers are built through a differential correction process briefly discussed hereafter.

IV.A.3. Differential correction process

For a given parameter set (Az, θ, d_M, ϕ), the A_{MH} is propagated backward in time from the halo orbit, on the stable manifold. From the final point on A_{MH} in the vicinity of the Moon, a tangential arrival at LEO

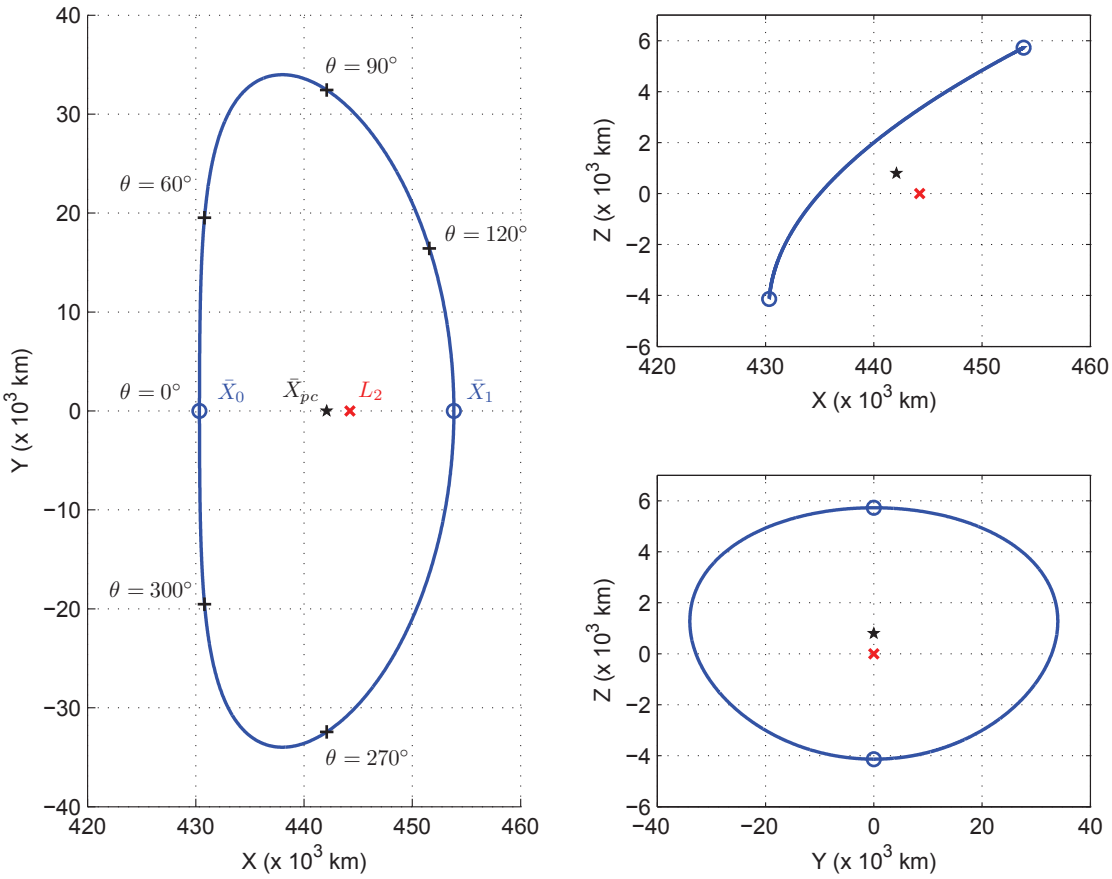

Figure 7: Position of the pseudo-center (black star) from three perspectives in the Earth-Moon reference frame for a given northern halo orbit with $Az = 5000\ km$. The EML_2 point (red cross) is also plotted, along with $\bar{X}_0$ and $\bar{X}_1$, the intersection points between the halo orbit and the x-axis (blue dots). The angle θ between the ($\bar{X}_{pc}$, $\bar{X}_0$) and ($\bar{X}_{pc}$, spacecraft) directions parametrizes the position of the spacecraft.

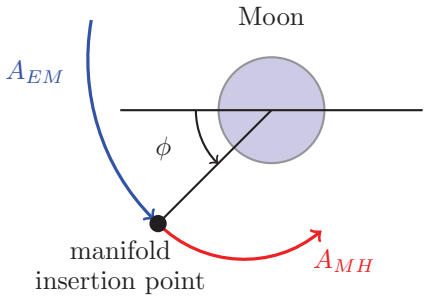

Figure 8: Definition of the angle ϕ in the case of an Earth-to-halo transfer. The angle ϕ positions the connection point between A_{MH} and A_{EM} with respect to the Moon.

is targeted using a numerical differential correction scheme such as the one developped by Gordon [4]. In this process, ΔV_{Mani} is iterated until a low-Earth orbit is reached. In this study, the tangency of ΔV_{Mani} is not imposed to ensure a more extensive possible solutions space.

The velocity of the spacecraft on the A_{MH} branch at the connection point between A_{EM} and A_{MH} is denoted V_{mani}. The initial velocity variation value used to start the iterative process is denoted ΔV_i. Figure 9 shows the different A_{EM} as a function of the ΔV_i for specific A_{MH} arcs, that is for $(Az, d_M, \phi) = (5000\ km, 50\ km, 45°)$ and for various values of θ. Though the direction of the maneuver is let free to vary in the differential correction process, the ΔV_i is chosen to be colinear to the velocity V_{mani} at the manifold

entrance point and is given in percentage of this velocity. From Figure 9a, it is clear that different values of ΔV_i lead to various types of A_{EM} solutions, each with specific values for ΔV_{LEO}, ΔV_{Mani}, the time of flight and the LEO latitude. In this way, even with all the design parameters (Az, θ, d_M, ϕ) fixed, multiple flyby trajectories can be computed, creating a family of solutions parametrized by ΔV_i. The transfer scenarios presented in the following sections are the result of arbitrary choices inside these families of solutions: the ΔV_i that produces the smallest maneuvers is selected. However, ΔV_{Mani} as a function of ΔV_i in Figure 9b shows complex behaviour with local minima and is highly dependant on the A_{MH} arc, which complicates the systematic selection of a good initial guess. Thus, for any given A_{MH} arc, the A_{EM} with the smallest maneuvers is selected through a grid search or a rough genetic algorithm.

The halo-to-Earth transfers are built with a similar process with a forward propagation of the equations of motion, with ϕ usually taken between $-90°$ and $0°$.

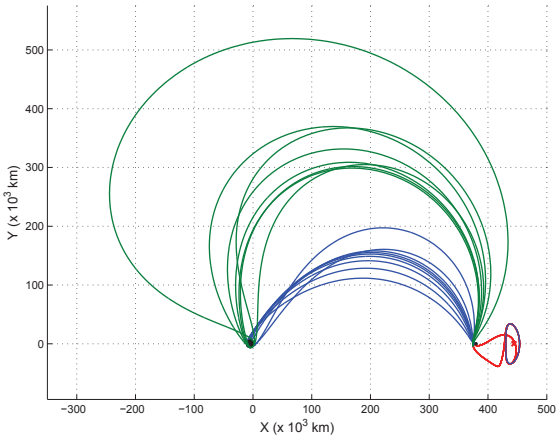

(a) Examples of families of orbits generated from specific A_{MH} arcs (in red) for various values of ΔV_i. In blue: $\theta = 95°$. In green: $\theta = 270°$

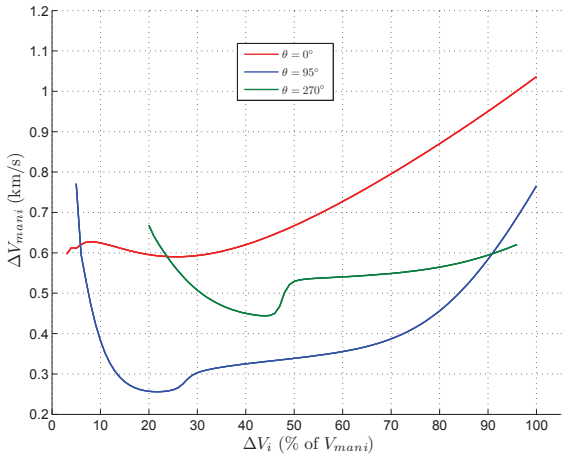

(b) ΔV_{Mani} as a function of ΔV_i taken as a percentage of the velocity V_{mani} at the manifold entrance point for specific values of θ.

Figure 9: Example of the influence of the initial velocity guess ΔV_i at manifold injection point on the trajectory A_{EM} and on the final maneuver ΔV_{Mani}. The results are shown for two specific A_{MH} arcs, defined by $(Az, d_M, \phi) = (5000\ km, 50\ km, 45°)$ and $\theta = 0, 95$ and $270°$.

At the end of the differential correction process, the low-Earth orbit and the boost ΔV_{Mani} are obtained. The ΔV_{LEO} maneuver is then calculated to make the link between the transfer trajectory and the circular LEO. The overall fuel cost is then given by the relationship $\Delta V_{\text{tot}} = \Delta V_{\text{Mani}} + \Delta V_{\text{LEO}}$.

IV.B. Evolution of the maneuvers and the time of flight with the design parameters (Az, θ, d_M, ϕ).

In the view of optimizing the transfers, the influence of key parameters on the maneuvers, the time of flight and the LEO latitude is discussed. Given the symmetry of the Earth-to-halo and halo-to-Earth transfers discussed in Section III.B, only the Earth-to-halo trajectories are studied in this section. Moreover, given that the variations of ΔV_{Mani} are clearly visible on the overall cost ΔV_{tot} [5], this section uses ΔV_{tot} as the unique characteristic quantity of the fuel consumption. Finally, the non-physical parameter d_M is fixed to 50 km.

IV.B.1. Evolution of fuel cost (ΔV_{tot})

In order to understand the influence of the design parameters on ΔV_{tot}, the following set of parameters has been fixed: $Az = 5000, 6000, \ldots 30000$ km, $\phi = 0, 10, \ldots 90°$, and $\theta = 1, 2, \ldots 360°$. Figure 10 shows the resulting costs ΔV_{tot} as a function of θ, for $Az = 5000$ km. For this example, the region of the orbit between $\theta = 102°$ and $\theta = 252°$ does not produce any viable trajectory because of a potential collision of the corresponding manifold branch with the Moon. This region is denoted "no-go window" in this study. For this Az value, and for any value of the parameter ϕ, one can see a significant drop of the cost in the vicinity

of the no-go window, which corresponds to the closest lunar flybys. This correlation between the overall cost and the distance to the Moon during the flyby is coherent with previous works [4, 16].

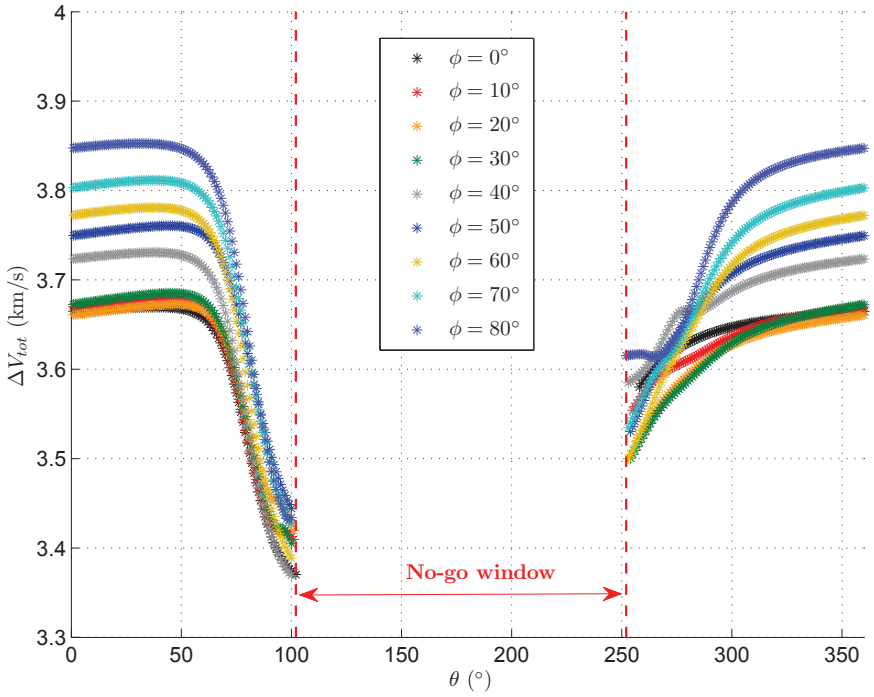

Figure 10: The overall transfer cost ΔV_{tot} of lunar flyby trajectories as a function of the position on the orbit θ for various values of ϕ. The out-of-plane amplitude Az is set to 5000 km. The no-go window is the region of the orbit between $\theta = 102°$ and $\theta = 252°$ that does not produce any viable trajectory because of a potential collision of the corresponding manifold branch with the Moon.

Moreover, one can see that, depending on the value of θ, the minimum cost may correspond to various values of ϕ. In order to cancel the influence of ϕ, for each value of θ the mininum value of ΔV_{tot} is selected in the field of variation of ϕ. The corresponding curves are plotted in Figure 11 for various values of Az between 4000 and 25000 km. For small Az values, the minimum ΔV_{tot} still corresponds to the closest lunar flybys, in the vicinity of the no-go window. However, it is the contrary for Az values greater than 10 000 km. The overall cost for a flyby trajectory to a halo orbit of $Az = 25000$ km is always greater than 3.6 km/s, whereas trajectories with a cost smaller than 3.35 km/s are possible if $Az = 4000$ km. This result illustrates the pertinence of the flyby strategy for orbits with small out-of-plan extensions, and symmetrically shows its irrelevance for greater Az values. In general, ΔV_{tot} is an increasing function of Az for almost all values of the position θ. In the light of these conclusions, the discussion is restricted to $Az \in [4000\ km, 15000\ km]$ for the rest of the article.

For a given halo orbit, the best solution in terms of ΔV_{tot} has been selected in the restricted pool $\phi = 0, 10, \ldots 90°$, and $\theta = 1, 2, \ldots 360°$. The overall cost ΔV_{tot} and the time of flight TOF of these trajectories are shown in Figure 12 for various value of the maximum out-of-plane amplitude Az, along with a plot of the best solution for $Az = 4000$ km. One can see that the minimum ΔV_{tot} is an increasing function of Az, which is in favor of the minimization of the halo orbit size.

We want to have a closer look on the circumstances of the flyby in the vicinity of the Moon for small Az values. To do so, we introduce the distance $d_{Moon,inj}$ which corresponds to the distance between the manifold injection point and the surface of the Moon. The angle α_{HM} of the lunar boost with respect to the velocity at the manifold injection point is also introduced. The value $\alpha_{HM} = 0°$ corresponds to a tangential maneuver. The $d_{Moon,inj}$ and α_{HM} values are then plotted for every mininum of ΔV_{tot}, regardless of the value of ϕ. The results are shown in Figure 13a and 13b. The smallest maneuvers are found for the smallest values of $d_{Moon,inj}$ and α_{HM}, which corresponds to very close lunar flybys with a quasi-tangential ΔV_{Mani} maneuver. This results is perfectly consistent with previous efforts [22]. However, one can see that neither a small distance to the Moon nor a quasi-tangential maneuver guarantees a small cost, since the corresponding

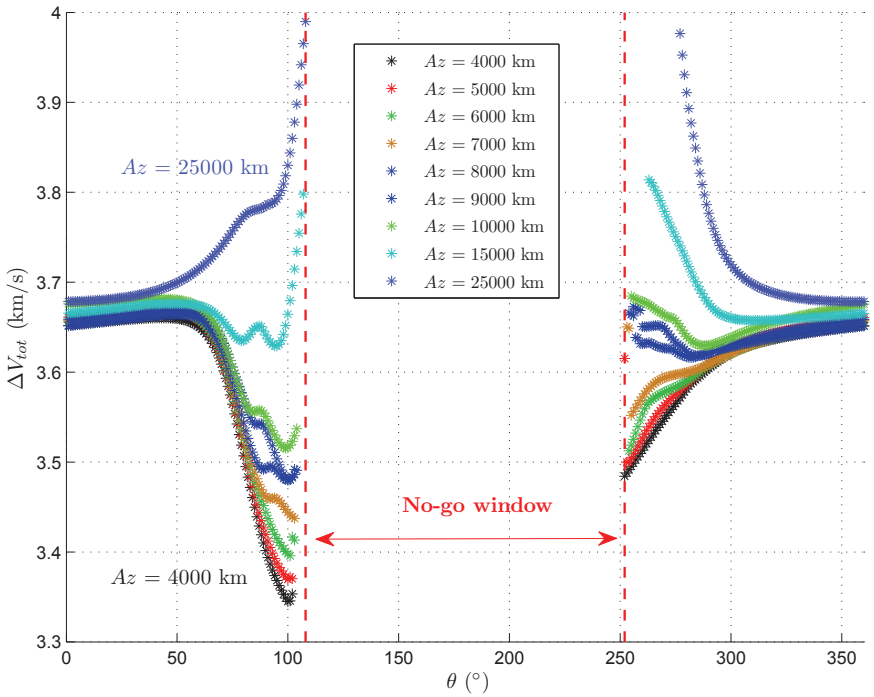

Figure 11: The minimum ϕ-independent overall cost ΔV_{tot} of lunar flyby trajectories as a function of the position on the orbit θ for various values of the out-of-plane amplitude Az.

functions are far from being bijective. Thus, in the context of an optimization of the fuel cost, one has to keep in mind that small values of $d_{Moon,inj}$ and α_{HM} should be targeted but they do not guarantee an optimized transfer. This is especially true for the dependance in α_{HM}, which validates the choice not to impose the tangency of the ΔV_{Mani} maneuver in the differential correction process, without any more information in the search space.

In the context of an optimization of the fuel cost, we have seen so far that the best results tend to be found for small values of Az and for close lunar flybys with tangential maneuver, which corresponds to positions on the halo orbit close to the no-go window. In the following section, the time of flight TOF is also considered in order to build the best trajectories both in terms of fuel cost and travel time.

IV.B.2. Relation between the fuel cost ΔV_{tot} and the time of flight TOF

In the view of manned spaceflight, this section focuses on the trade-off between the fuel and the time costs. To do so, the overall time of flight (TOF) is computed for the set of trajectories defined in the previous section. Figure 14 shows the scatter diagram of (ΔV_{tot},TOF) for $Az = 5000$ km and for various values of ϕ. Regardless of the value of ϕ, the best trajectories (cyan circles) are situated in the lower left corner of the figure, as both small ΔV_{tot} and time of flight are sought. These trajectories creates a Pareto front in the (ΔV_{tot}, TOF) space that can be computed for any orbit with small out-of-plane amplitudes. The corresponding results are presented in Figure 15 for various values of Az. In this figure, the trade-off between the fuel cost and the time of flight is apparent. The fastest transfers (less than 19 days of travel for $Az = 7000$ km) are obtained thanks to the highest maneuvers (more than 3.7 km/s for $Az = 7000$ km) and conversely. The shortest transfers are obtained for $Az = 7000$ km, the most fuel efficient for $Az = 4000$ km.

The derivative ΔV_{tot} with respect to the time of flight is noted $D_{\text{T}}\Delta V_{\text{tot}}$. In the range [18.5 days, 20 days], $D_{\text{T}}\Delta V_{\text{tot}}$ is highly negative, typically between -52 and -27 m/s/day. For a time of flight greater than 20 days, $D_{\text{T}}\Delta V_{\text{tot}}$ is less than 8 m/s/day. Thus, there is a twist in the trade-off situation around the 20-days value: it is much more time consuming to reach the minimum ΔV_{tot} in the long-flight region than to save fuel in the short-flight range. The best trade-offs correspond to a time of flight around 20 days and an overall fuel cost around 3.45 km/s.

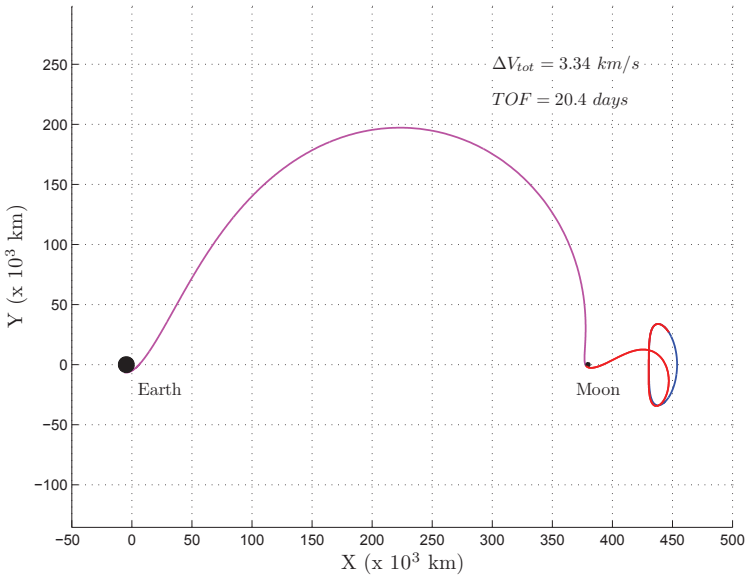

Az (km)	ΔV_{tot} (km/s)	TOF (days)
4000	3.34	20.4
5000	3.36	20.1
6000	3.39	21.8
7000	3.44	21.3
8000	3.48	21.3
9000	3.48	21.3
10000	3.52	19.2

Figure 12: The best solutions in terms of ΔV_{tot} has been selected in the restricted pool $\phi = 0, 10, \ldots 90°$, and $\theta = 1, 2, \ldots 360°$. Left panel: the best solution in the XY-plane of the Earth-Moon reference frame for $Az = 4000$ km. The A_{EM} arc is in magenta, the A_{MH} arc in red. Right panel: the overall cost ΔV_{tot} and the time of flight TOF.

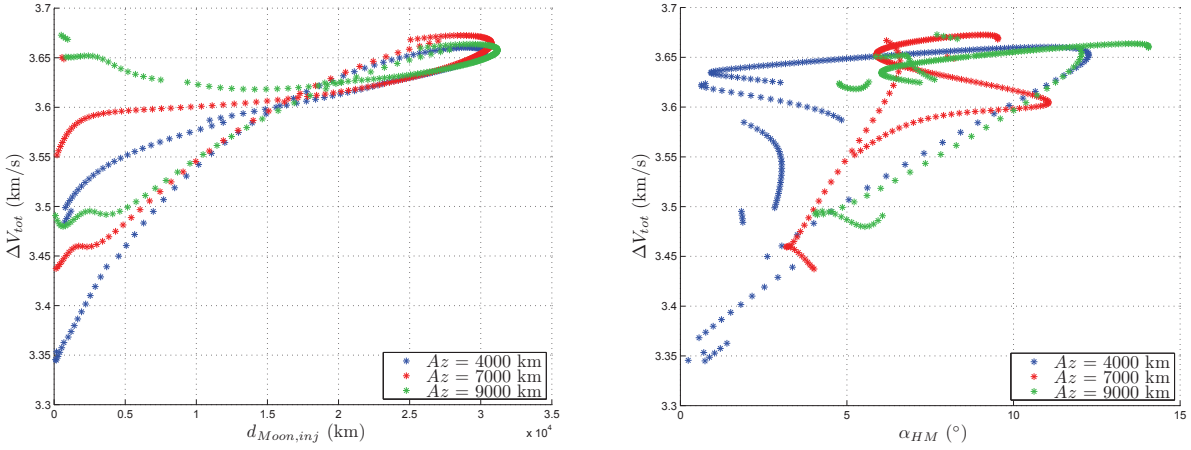

(a) ΔV_{tot} as a function of $d_{Moon,inj}$

(b) ΔV_{tot} as a function of α_{HM}

Figure 13: Influence of the circumstances of the lunar flyby on the minimum ϕ-independent overall cost ΔV_{tot} for various values of the out-of-plane amplitude Az. Two parameters are considered: the distance $d_{Moon,inj}$ which corresponds to the distance between the point of injection in the manifold and the surface of the Moon and the angle α_{HM} of the lunar boost with respect to the velocity at the manifold injection point.

IV.B.3. Latitude of the low-Earth parking orbit

The latitude of the parking orbit is let free to vary in the differential correction process used to compute the trajectories. However, the spacecraft is initially injected into near-Earth space at a latitude restrained by the performances of its launcher and the situation of the spaceport. Thus, an additional maneuver may be required to reach the parking orbit from the original orbit of insertion. To reduce the cost of this maneuver, the latitude of insertion of the spacecraft needs to be close to the latitude of departure from Earth, which constrains the latitude of the spaceport. This section aims to quantify the range of variation of the latitude of the parking orbit to have an estimation of the most suitable spaceport. It is calculated at the position

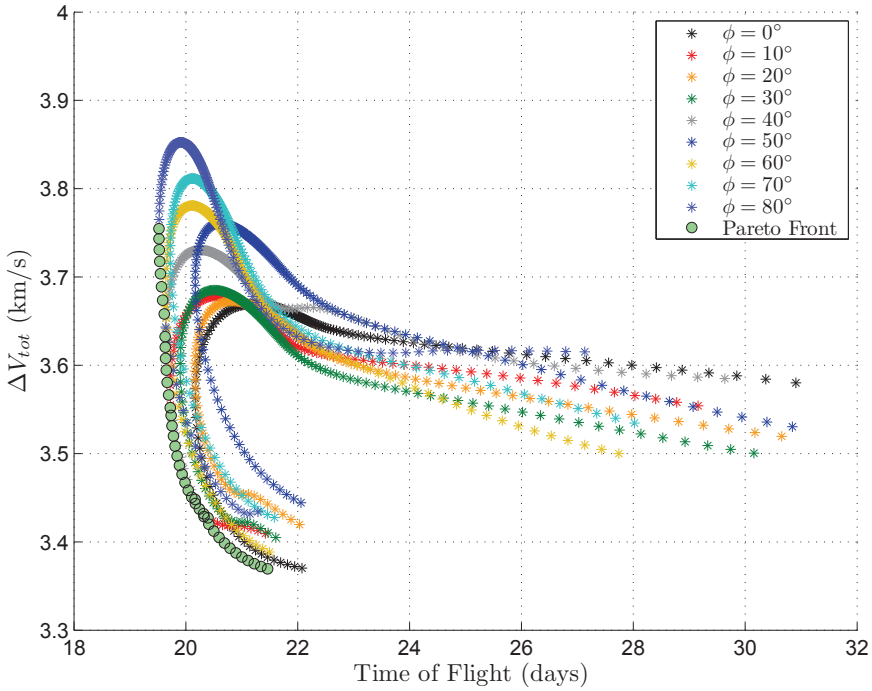

Figure 14: Scatter diagram of (ΔV_{tot},TOF) for Az = 5000 km and for various values of ϕ. The best trajectories (cyan circles) are situated in the lower left corner of the figure, as both small ΔV_{tot} and time of flight are sought. These trajectories creates a Pareto front in the (ΔV_{tot}, TOF) space.

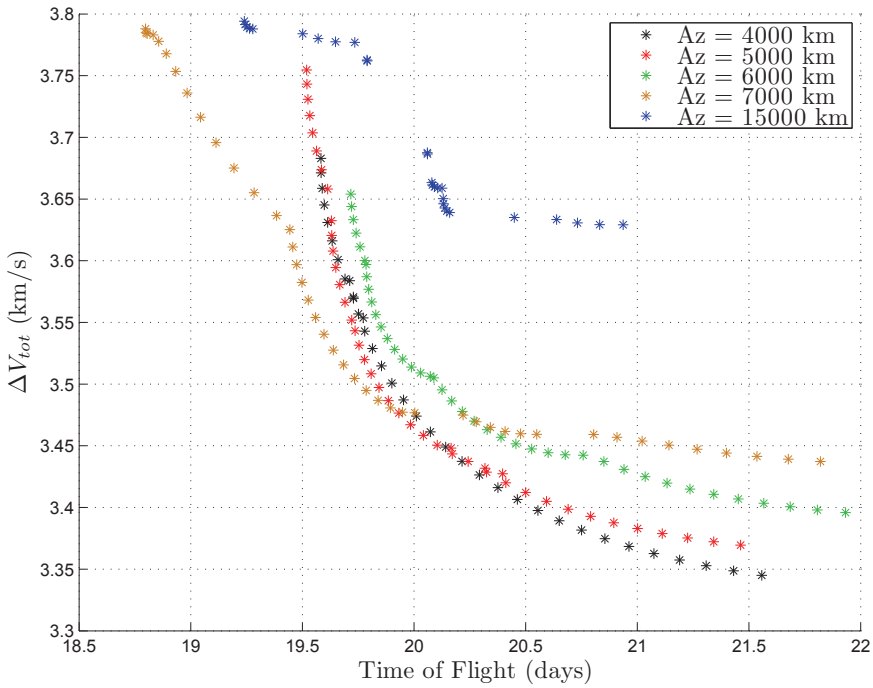

Figure 15: The ϕ-independant best trajectories in the (ΔV_{tot}, TOF) space, for various values of Az. One can see that there is a twist in the trade-off situation around the 20-days value: it is much more time consuming to reach the minimum ΔV_{tot} in the long-flight region than to save fuel in the short-flight range.

of the LEO boost and takes into account the obliquity of the Earth and the inclination of the Earth-Moon plane with respect to the ecliptic. Similarly to Section IV.B.1, for each value of θ, the minimum of ΔV_{tot}

and the corresponding Earth latitude are selected in the field of variation of ϕ. The results are shown in Figure 16 for various values of the out-of-plane amplitude Az. The average latitude is 28° for every Az, which roughly corresponds to an low-Earth orbit into the Earth-Moon plan. The deviation range around this value is about $[-2°, +4°]$ with a standard deviation of 1.4 for $Az = 4000$ km and $[-2°, +9°]$ with a standard deviation of 2.2 for $Az = 15000$ km. The latitude of the low-Earth orbit is then close to 28° for every flyby trajectories of interest. This latitude has to be reached by the spacecraft from the insertion orbit of its launcher. With its latitude of 28°31′, the Kennedy Space Center would allow the insertion orbit to be very close to the parking orbit, and thus can be considered as the most suitable spaceport for this type of mission.

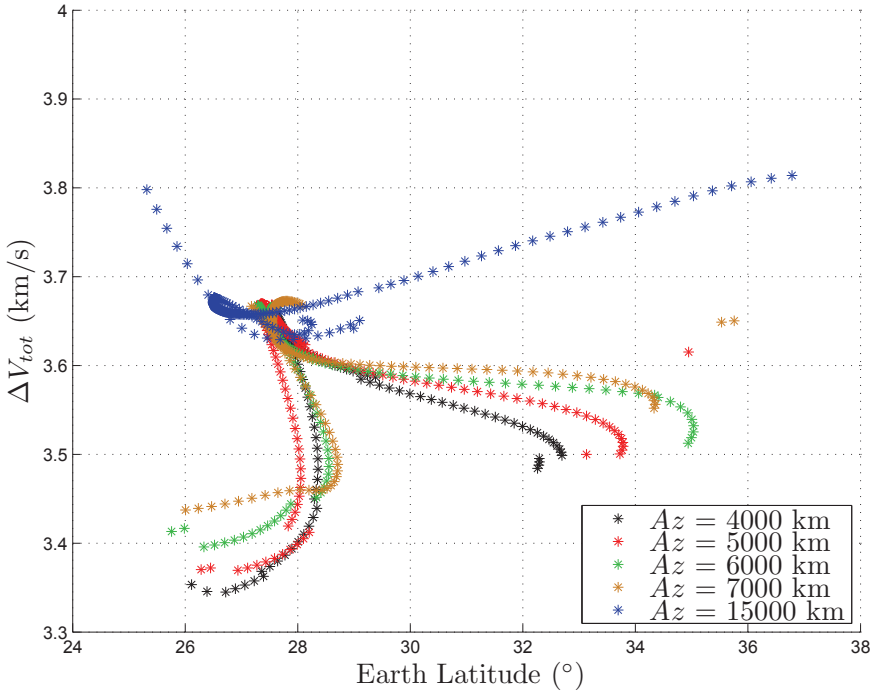

Figure 16: The minimum ϕ-independent overall cost ΔV_{tot} as a function of the latitude of the low-Earth parking orbit for various values of the out-of-plane amplitude Az.

IV.C. The no-go window of halo-to-Earth and Earth-to-halo transfers

For a given position of the spacecraft on the halo orbit defined by (Az, θ), the A_{MH} computed with the parameters (d_M, ϕ) may collide with the Moon, therefore leading to an unrealistic trajectory. This type of collision is usually obtained for a continuous range of position on the orbit, both for the stable and unstable manifolds i.e. for both traveling directions. This range, noted $[\theta_1, \theta_2] \subset [0, 360°]$ defines the "no-go window" of halo-to-Earth and Earth-to-halo transfers. This window imposes constraints on the mission design: for Earth-to-halo transfers, the set of halo injection points at a given date may be restricted; for halo-to-Earth transfers, flyby strategies may be impossible for certain positions and dates. This section aims to investigate the structure of the no-go window and introduce its influence on mission design. Given the symmetry of the Earth-to-halo and halo-to-Earth transfers, only halo-to-Earth trajectories are studied in this section. For the purpose of this study, the temporal extent of the no-go window is denoted as T_{nogo} and is given as a fraction of the orbital period T_0.

IV.C.1. The influence of d_M on the no-go window

As stated in Section IV.A.2, d_M can be considered as a design parameter, despite its non-physical nature. Given the asymptotic behavior of the motion in the vicinity of the halo orbit, manifolds are not propagated directly from a position on the orbit: the starting point is taken at the distance d_M in the initial stable or unstable direction given by linear approximation. The motion of the spacecraft on the manifold and thus the

position and amplitude of the no-go window are very sensitive to the d_M value. Figure 17 shows the spatial and temporal extent of the no-go window as a function of d_M for $Az = 4000$ km and for the median value $\phi = -45°$. One can see that the duration of the window is very variable for small values of d_M, ranging between 20 and 30 % of the orbital period for this example. Figure 17a shows that the no-go window is also spatially variable and "moves" on the orbit along with d_M. Complementary studies should be carried out to characterize more precisely the influence of d_M on the no-go window and the overall mission design. In the meantime, d_M has been fixed to an arbitrary value of 50 km to cancel out its effect.

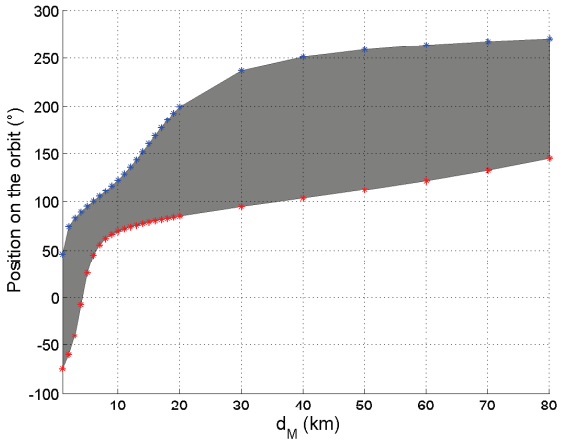

(a) The spatial extent (in grey) of the no-go window as a function of d_M.

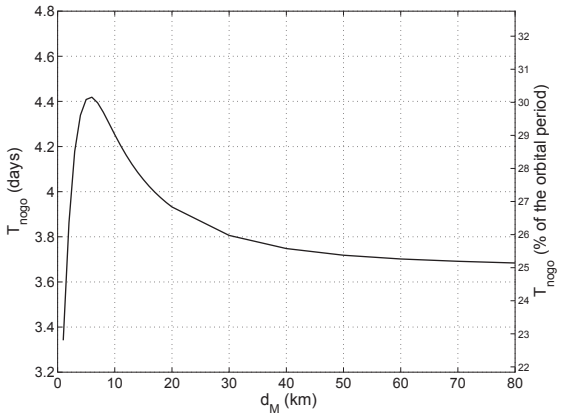

(b) The temporal extent T_{nogo} of the no-go window as a function of d_M. The results are given in days and in percentage of the orbital period.

Figure 17: The spatial and temporal extent of the no-go window as a function of d_M for $Az = 4000$ km and for the median value $\phi = -45°$. On the left panel, the spatial extent is represented by the values θ_1 (in red) and θ_2 (in blue) which are taken in $\mathbb{R}$ instead of $[0, 360°]$ to ensure continuity. The continuous range for which flyby transfers are impossible is in grey.

IV.C.2. Influence of the no-go window on return missions

For a given position on the orbit, a return flyby strategy from the station may be impossible to implement if it interferes with the no-go window. We aim to quantify the delay induced by the presence of the no-go window on the return strategy. For a given set of the parameters (Az, d_M, ϕ), the fastest halo-to-Earth transfer has been computed for $\theta = 1, 2, \ldots 360°$ with the scheme described hereafter. For a given position θ_0, the initial transfer is the classical flyby transfer with θ_0 taken as the departure point, with a time of flight $T_{transfer,0}$. For all the positions $\theta_i = 1, 2, \ldots 360°$ the duration $T_{orbit,i}$ of the orbit arc between θ_0 and θ_i is computed. The time of flight of the classical flyby transfer with θ_i taken as the departure point, is denoted $T_{transfer,i}$. The fastest halo-to-Earth transfer at θ_0 is then given by the minimum $\min_{\theta_i}(T_{orbit,i} + T_{transfer,i})$ with the departure point $\arg\min_{\theta_i}(T_{orbit,i} + T_{transfer,i})$. The resulting return mission durations are presented in Figure 18 for (Az, d_M, ϕ) = (5000 km, 50 km, 45°). As expected, the no-go window almost doubles the maximum mission duration. Quantitatively, at the beginning of the window, 48 days are needed to go back to Earth if a flyby return is decided. Thus, in the context of crew safety, other strategies than flyby have to be implemented to meet the requirements of quick return from the station.

V. Station deployment and cargo missions trajectories

In this section, we will focus on another kind of trajectories. The setting-up of a habitable station on a halo orbit would imply one or several deployment missions and regular cargo flights to resupply the astronauts in food, water and other consumables. The main criterion of selection for these unmanned missions is the cost reduction in terms of propellant whereas longer trip durations can be accepted. Consequently, a WSB strategy is selected, which enables the most efficient trips.

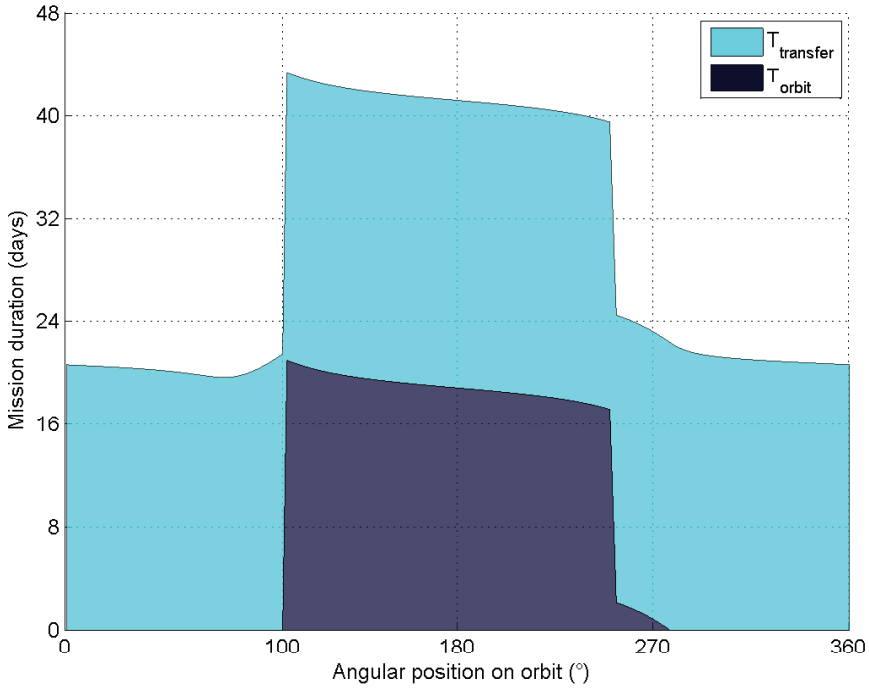

Figure 18: The fastest halo-to-Earth flyby strategy as a function of the current position θ for (Az, d_M, ϕ) = (5000 km, 50 km, 45°). In deep blue: T_{orbit} the time spent on the halo orbit before departure. In light blue: $T_{transfer}$ the duration of the transfer to LEO.

V.A. Transfer strategy to EML_2 halo orbit

In the WSB strategy, two CR3BP are patched, the Sun-Earth CR3BP and the Earth-Moon CR3BP. This strategy consists in reaching a Sun-Earth low-energy trajectory with a first LEO maneuver, and then entering the Earth-Moon stable manifold with or without a second maneuver.

The transfer is divided into two artificial phases. The first one leads the spacecraft from its departure LEO to the entrance point of the Earth-Moon stable manifold whereas the second one consists in the asymptotic drifting along the manifold to the final halo orbit. In order to benefit from the solar dynamical assistance, the first stage is calculated in the Sun-Earth CR3BP, which means the influence of the Moon is not taken into account. The initial low-Earth orbit is chosen to lie in the ecliptic, thus the first leg of the trajectory is contained in the $z = 0$ plane. On the contrary, the second part of the trajectory is calculated in the Earth Moon CR3BP so that the stable manifold is used to reach the halo orbit. Following the work of [19], two Poincaré sections, namely P_{SE} and P_{EM} are generated to detect connections between the two legs of the trajectory. They are defined in Figure 19, along with their associated angles ϕ_{SE} and ϕ_{EM}. The design of the whole Earth-to-halo trajectory comes down to the selection of pairs of intersection points $\mathbf{y}_{SE} \in P_{SE}$ and $\mathbf{y}_{EM} \in P_{EM}$.

V.A.1. Conditions of feasibility for the Earth-to-halo connection

The necessary condition to identify feasible trajectories is the coincidence, at least in the configuration space, of the points $\mathbf{y}_{SE}$ and $\mathbf{y}_{EM}$. That first requires the two surfaces of section P_{SE} and P_{EM} to project on the same line in the (x,y) plane. In terms of mutual positioning of the primaries, it means that the Earth-Moon line must be tilted by the angle $\beta = \phi_{SE} - \phi_{EM}$ with respect to the Sun-Earth line at the time the spacecraft is on the section (see Figure 19). Moreover, since the Poincaré map P_{SE} lives in the $z = 0$ plane, the search of possible intersections is restricted to the two points in P_{EM} with zero z-coordinate. Since the spatial flow is never tangential to the $z = 0$ plane, and although it is possible to achieve satisfying intersections in configuration space between P_{SE} and $P_{EM} \cap \{z = 0\}$, a small out-of-plane component of the velocity maneuver can never be avoided.

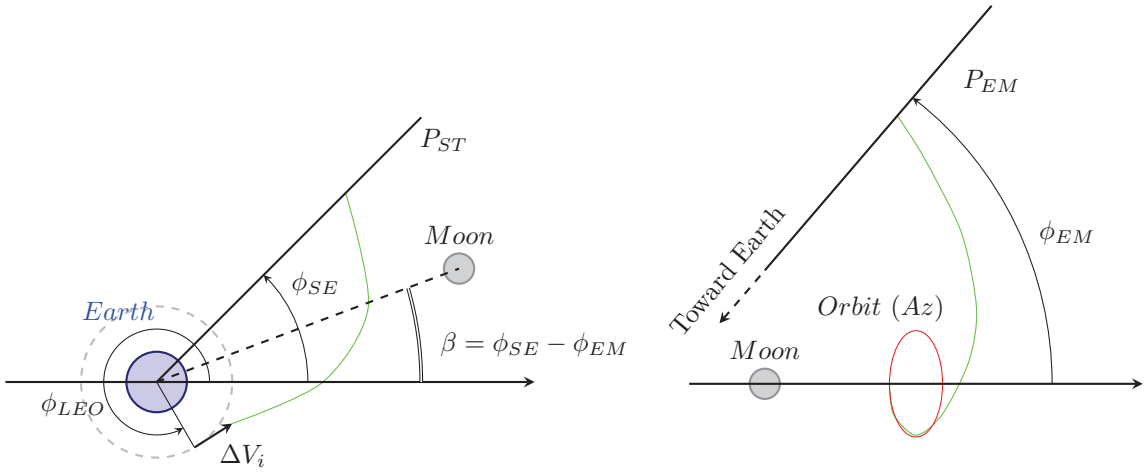

(a) Earth escape trajectory (Sun-Earth system). (b) Halo arrival trajectory (Earth-Moon system).

Figure 19: Definition of the optimization parameters for the patched Three-body problem.

Candidate pairs of transfer points have to be selected by efficiently varying the following design parameters in their range of definition (adapted from [19]):

- $\phi_{LEO} \in [0, 360°]$: the departure angle on LEO;
- $\Delta V_i \in [3150, 3250\ m/s]$: the first thrust needed to leave LEO;
- $\phi_{SE} \in [0, 180°]$: the angle between the x-axis and the Poincaré plane P_{ST} in the Sun-Earth system;
- $\phi_{EM} \in [0, 180°]$: the angle between the x-axis and the Poincaré plane P_{EM} in the Earth-Moon system;
- $Az \in [4000, 30000\ km]$: the out-of-plane amplitude of the halo orbit.

As in Section IV.A.2, departure LEO altitude h_{LEO} of 200 km has been selected.

For any pair $\mathbf{y}_{SE} = \{x_{SE}, y_{SE}, z_{SE}, \dot{x}_{SE}, \dot{y}_{SE}, \dot{z}_{SE}\}$ and $\mathbf{y}_{EM} = \{x_{EM}, y_{EM}, z_{EM}, \dot{x}_{EM}, \dot{y}_{EM}, \dot{z}_{EM}\}$, the conditions for a successful connection are defined by:

$$\left\| \begin{pmatrix} x_{SE} \\ y_{SE} \end{pmatrix} - \begin{pmatrix} x_{EM} \\ y_{EM} \end{pmatrix} \right\| \leq 10\ km$$

$$\left\| \begin{pmatrix} \dot{x}_{SE} \\ \dot{y}_{SE} \\ \dot{z}_{SE} \end{pmatrix} - \begin{pmatrix} \dot{x}_{EM} \\ \dot{y}_{EM} \\ \dot{z}_{EM} \end{pmatrix} \right\| \leq 30\ m/s$$

V.A.2. Search algorithm

Given the high number of parameters, the search algorithm has been divided in two steps. First, a couple (Az,ϕ_{EM}) is selected to define the manifold leg of the trajectory. The corresponding intersection points of the halo manifold with both the Poincaré plane and the $z = 0$ plane are calculated. Then, for the Earth leg, a rough search in the $\{\phi_{SE}, \phi_{LEO}, \Delta V_i\}$ space showed that, on average, only one combination of these 3 parameters satisfy the previous conditions. Therefore, an optimization algorithm based on the three variables $\{\phi_{SE}, \phi_{LEO}, \Delta V_i\}$ is implemented.

This problem being highly nonlinear, a classical multi-objective genetic algorithm has been used to look for parameters minimizing both the position gap and the velocity gap between the two legs of the trajectory. A database of manifold entrance points has been built for three different Az by exploring the interval of ϕ_{EM} from 10° to 170° with a step of 0.1°. The genetic algorithm has then been run to access each of these points starting from LEO. After the maximum number of iterations has been reached, only optimized trajectories satisfying the conditions of successful connection have been kept.

V.B. Results

The operational features of the calculated trajectories are shown in Figure 20. The cost of a trajectory is measured by the total change of velocity ΔV_{tot} required along the entire trajectory, i.e. the sum of the initial impulsion in LEO and the velocity gap at the intersection of the two legs.

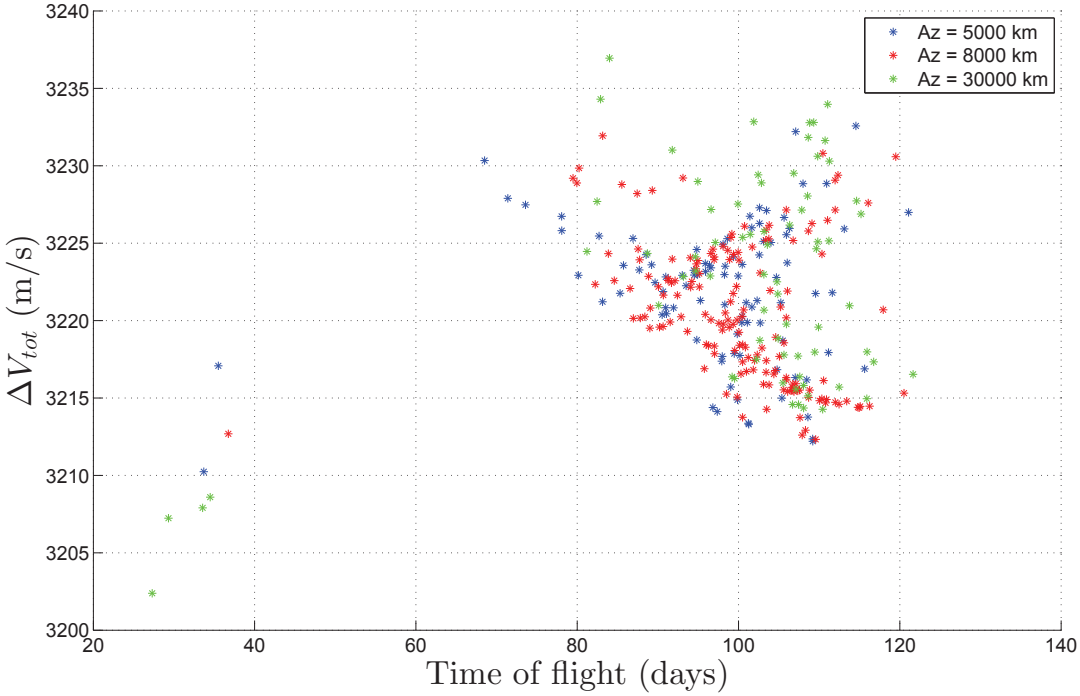

Figure 20: Performance of the WSB trajectories obtained by the genetic algorithm and satisfying the conditions of successful connection: total ΔV required in function of time of flight.

We observe that most trajectories can be grouped together in what we will call the nominal family in the rough range $[3210, 3235]$ m/s $\times[70, 120]$ days, corresponding to the data found in the literature (see Table 1). One of them is traced in Figure 21. A few unexpected trajectories are found around a time of flight of 35 days. An example of these second type trajectories is shown in Figure 22. The velocity change at the intersection is significant in direction but the gap of speed satisfies the above conditions of successful connection. Further studies should be carried out to check the relevance of such solutions. If their existence were to be confirmed, they would represent very attractive transfer solutions given their short duration. As for now, without any complementary validation, we decide to discard them.

The analysis of Figure 20 shows that the amplitude Az has a minor influence on the performance inside the nominal family, whereas large Az reduce the cost of type 2 trajectories. However the influence of this parameter is much less significant than the one of h_{LEO}. Indeed, a similar optimization problem has been set up for $h_{LEO} = 400$ km and $Az = 8000$ km and gave the best ΔV_{tot} at 3163 m/s. All these transfers are reproducible every lunar period of rotation, providing mission designers with an extensive pool of solutions to reach the halo orbit. One may notice that the genetic algorithm finds twice as many satisfying trajectories for $Az = 8000$ km as for the two other orbit amplitudes.

A deeper look at the obtained distribution of the design parameters points out that there exists a preferential relation between ϕ_{LEO} and ϕ_{SE}, as shown in Figure 23. The trajectories can be divided into two groups according to their starting zone. The main one regroups transfer legs shooting from around $\phi_{LEO} = 330°$, i.e. the LEO opposite-to-the-Sun side (see Figure 24), in direction of the first Sun-Earth Lagrangian point SEL_1, and meeting the Poincaré map at an average $\phi_{SE} = 160°$. This group also contains the type 2 fast trajectories identified earlier. The second solution consists in starting from around $\phi_{LEO} = 330°$ and in shooting toward SEL_2. The relative importance of the first group suggests to preferentially try to take advantage of the SEL_1 dynamics.

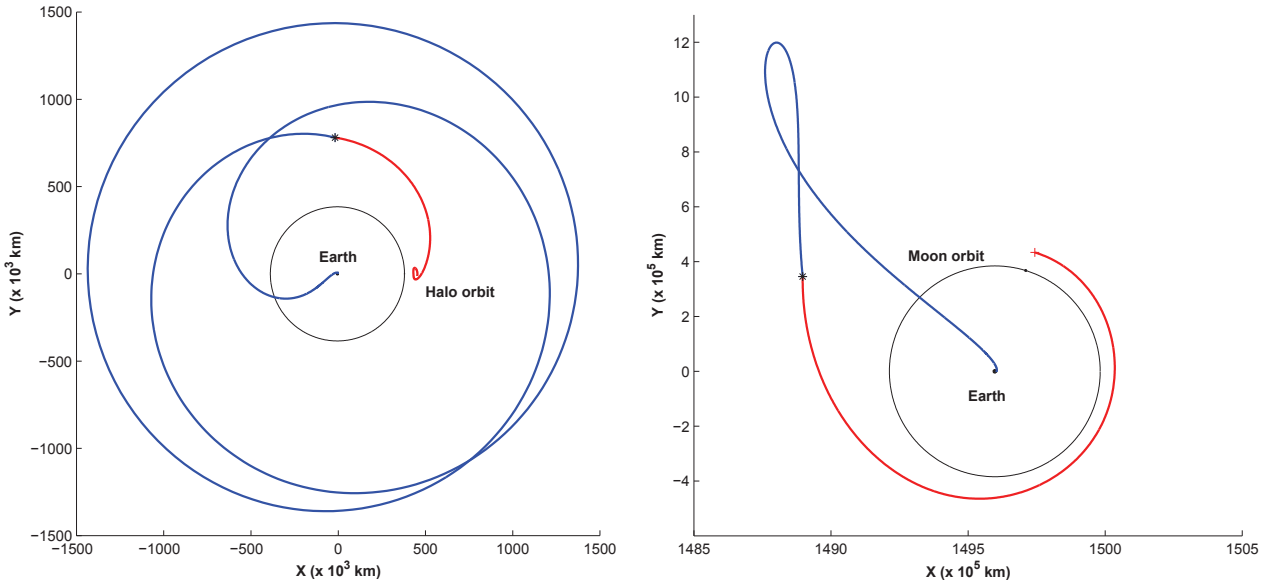

(a) Trajectory in Earth-Moon rotating frame.

(b) Trajectory in Sun-Earth rotating frame.

Figure 21: Earth-to-halo trajectory from nominal family, for a final orbit of $Az = 8000\ km$. The time of flight is about 102 days, the global ΔV is $\Delta V_{tot} = 3220\ m/s$, the velocity gap at the connection point is $\Delta V_{gap} = 4\ m/s$. In blue: Earth departure leg. In red: halo arrival leg.

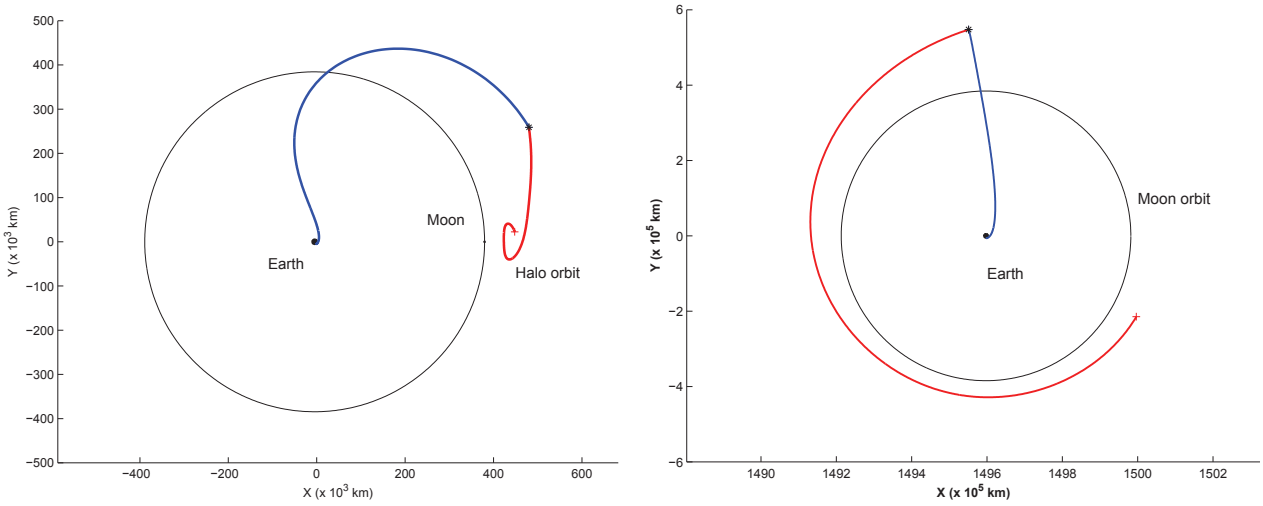

(a) Trajectory in Earth-Moon rotating frame.

(b) Trajectory in Sun-Earth rotating frame.

Figure 22: Earth-to-halo trajectory of type 2, for a final orbit of $Az = 30000\ km$. The time of flight is about 29 days, the global ΔV is $\Delta V_{tot} = 3207\ m/s$, the velocity gap at the connection point is $\Delta V_{gap} = 28\ m/s$. In blue: Earth departure leg. In red: halo arrival leg.

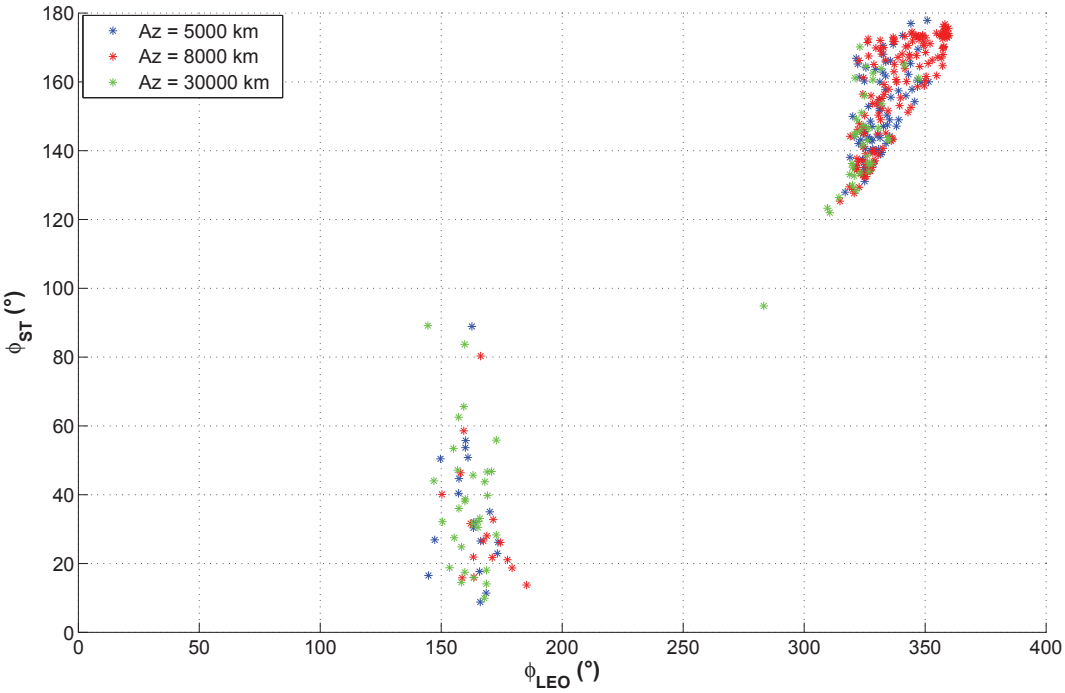

Figure 23: Distribution of ϕ_{LEO} and ϕ_{SE} for every satisfying WSB trajectories.

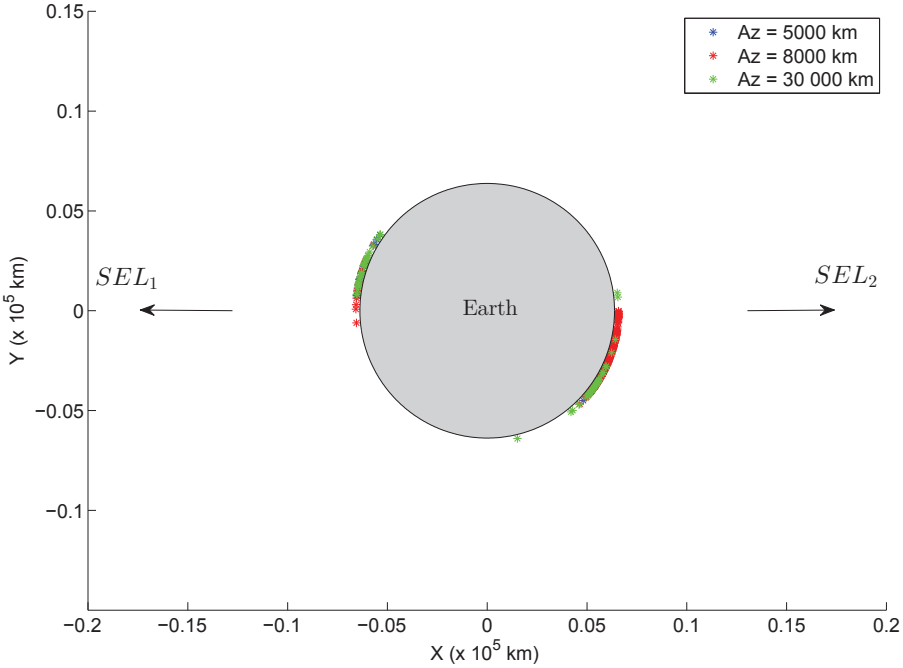

Figure 24: Starting points on LEO for every satisfying WSB trajectories. Right (resp. left) group of points shoot in direction of SEL_1 (resp. SEL_2). In grey: Earth.

If, beyond the domain of mission design, a better precision on the ΔV cost is needed, a decisive step

would consist in computing more physical solutions in a 4-body problem that would take into account the influence of the Sun and the Moon on both legs of the transfer, by using the previous trajectories obtained in the CR3BP as first guesses. The addition of the Moon in the simulation of the departure leg would modify its shape in the lunar vicinity, but literature [4, 14] has shown that the calculated order of magnitude for the thrust needed and time of flight would remain close to the new values. It would also be interesting to see if the type 2 fast trajectories still exist in such a more detailed model, or whether they are just an artifact tied to the simple CR3BP.

VI. Conclusions and prospects

According to the ISECG roadmap, a research team at ISAE/SUPAERO is working on the mission analysis of an inhabited space station, orbiting around EML_2 on a halo orbit, so as to provide a safe outpost for human exploration. The main goal of this study is to compute and analyze optimized transfers from a LEO to the station orbit in the perspective of cargo missions and manned flights.

The bibliographic research pointed out many possible strategies in order to access a halo orbit around EML_2. We selected the most suitable among them, adapted to the requirements of each mission.

A deep space habitat would require frequent manned transfers between low-Earth orbit and the station. This type of mission demands a trade-off between the propellant consumption and the time of flight. Flyby strategies have been selected as the most suitable method for such a compromise. After an analysis of the design parameters of flyby trajectories on the fuel and time cost, the best results tend to be found for small values of the out-of-plane amplitude Az, for close lunar flybys, and for a tangential flyby maneuver. Moreover, a trade-off zone has been identified which corresponds to a time of flight around 20 days and an overall cost of 3.45 km/s. However, trajectories with cost as low as 3.34 km/s have been computed for small Az values.

The setting up of the station would also imply deployment missions and regular cargo flights to resupply the astronauts in consumables. The corresponding suitable trajectory would have very low cost in terms of propellant but would tolerate a longer trip duration, which justifies the selection of WSB strategy. The average performance of these trajectories is around 3.22 km/s with a time of flight of 100 days. The analysis of the data has shown that there exist a great number of launch possibilities every period of lunar rotation and that the dynamics of SEL_1 seems the most effective to exploit. The transition to a more complete 4-body problem would increase the precision of the performance and solve the question of the actual reality of the unexpected fast trajectories.

For future work, we will focus on other steps of the station deployment scenario. Based on the obtained results for ΔV and time of flight, detailed analysis of the space rendezvous issue on the halo orbit will be carried out. The study of elements prior to the transfer such as the launcher selection or the injection and features of the parking LEO orbit would also be worthy of interest.

References

[1] International Space Exploration Coordination Group, *The Global Exploration Roadmap*, 2011.

[2] S. Lizy-Destrez and C. Blank, "Mission analysis for a space medical center of an exploration gateway at lunar libration point," 2011.

[3] R. W. Farquhar, D. W. Dunham, Y. Guo, and J. V. McAdams, "Utilization of libration points for human exploration in the Sun–Earth–Moon system and beyond," *Acta Astronautica*, vol. 55, pp. 687–700, 2004.

[4] D. P. Gordon, "Transfers to Earth–Moon L2 Halo orbits using lunar proximity and invariant manifolds," Master's thesis, School of Aeronautics and Astronautics, Purdue University, West Lafayette, Indiana, 2008.

[5] E. M. Alessi, G. Gomez, and J. J. Masdemont, "Two-manoeuvres transfers between LEOs and Lissajous orbits in the Earth–Moon system," *Advances in Space Research*, vol. 45, pp. 1276–1291, 2010.

[6] H. Renk, F., "Exploration Missions in the Sun–Earth–Moon System: A Detailed View on Selected Transfer Problems," *Acta Astronautica*, vol. 67, pp. 82–96, 2010.

[7] V. Szebehely, *Theory of Orbits: The Restricted Problem of Three Bodies*. Academic Press, Inc., New York, New York, 1967.

[8] W. S. Koon, M. W. Lo, J. E. Marsden, and D. R. Shane, *Dynamical Systems, the Three-Body Problem and Space Mission Design*. Marsden Books, 2008.

[9] R. W. Farquhar, "The Utilization of Halo Orbits in Advanced Lunar Operations," Tech. Rep. X-551-70-449, NASA, Goddard Space Flight Center, December.

[10] E. Canalias, G. Gomez, M. Marcote, and J. Masdemont, "Assessment of mission design including utilization of libration points and weak stability boundaries," *ESA Advanced Concept Team*, 2004.

[11] R. R. Rausch, "Earth to Halo Orbit transfer trajectories," Master's thesis, School of Aeronautics and Astronautics, Purdue University, West Lafayette, Indiana, 2005.

[12] K. C. Howell, "Three–Dimensional, Periodic, Halo Orbits," *Celestial Mechanics*, vol. 32, pp. 53–71, 1984.

[13] D. L. Richardson, "Analytical construction of periodic orbits about the collinear points," *Celestial Mechanics*, vol. 22, pp. 241–253, 1980.

[14] C. E. Patterson, "Representations of invariant manifolds for applications in system-to-system transfer design," Master's thesis, School of Aeronautics and Astronautics, Purdue University, West Lafayette, Indiana, 2004.

[15] F. Bernelli-Zazzera, F. Topputo, and M. Massari, "Assessment of mission design including utilization of libration points and weak stability boundaries," *Ariadna Study id*, vol. 3, no. 4103.2004, 2004.

[16] L. Mingtao and Z. Jianhua, "Impulsive lunar Halo transfers using the stable manifolds and lunar flybys," *Acta Astronautica*, vol. 66, pp. 1481–1492, 2010.

[17] A. Miele, "Theorem of image trajectories in the Earth-Moon space," *Boeing Scientific Research Laboratories*, 1960.

[18] A. Miele and S. Mancuso, "Optimal trajectories for Earth–Moon–Earth flight," *Acta Astronautica*, vol. 49, no. 2, pp. 59–71, 2001.

[19] A. Zanzottera, G. Migotti, R. Castelli, and M. Dellnitz, "Intersecting invariant manifolds in spatial restricted three-body problems: Design and optimization of Earth-to-halo transfers in the Sun–Earth–Moon scenario," *Commun Nonlinear Sci Numer Simulat*, vol. 17, pp. 832–843, 2012.

[20] J. S. Parker, *Low-energy ballistic lunar transfers*. ProQuest, 2007.

[21] F. Topputo, M. Vasile, and F. Bernelli-Zazzera, "Earth-to-Moon Low Energy Transfers Targeting L1 Hyperbolic Transit Orbits," *Annals of the New York Academy of Sciences*, vol. 1065, no. 1, pp. 55–76, 2005.

[22] J. S. Parker and G. H. Born, "Direct Lunar Halo Orbit Transfers," *The Journal of the Astronautical Sciences*, vol. 56(4), pp. 441–476, 2008.